Cellular Physiology and Biochemistry

Cell Physiol Biochem 2018;50:2341-2364
DOI: 10.1159/000495096
Published online: 13 November 2018
Accepted: 5 November 2018

Original Paper

Peperomin E Induces Promoter Hypomethylation of Metastatic-Suppressor Genes and Attenuates Metastasis in Poorly Differentiated Gastric Cancer

Xin-zhi Wang[a] Jia-li Gu[b] Ming Gao[a] Yong Bian[a] Jiang-yu Liang[c] Hong-mei Wen[a] Hao Wu[a]

[a]School of Pharmacy, Nanjing University of Chinese Medicines, Nanjing, [b]Nanjing University of Science and Technology Hospital, Nanjing University of Science and Technology, Nanjing, [c]Department of Natural Medicinal Chemistry, China Pharmaceutical University, Nanjing, China

Key Words
Peperomin E • Gastric cancer • Metastasis • DNA methyltranferase inhibition • AMPKα-Sp1 signaling • Metastatic-suppressor gene

Abstract
Background/Aims: Peperomin E (PepE), a natural secolignan isolated from the whole plant of *Peperomia dindygulensis*, has been reported by ourselves and others to display potent anti-cancer effects in many types cancer cells, especially gastric cancer. However, the effects of PepE on the metastasis of poorly-differentiated gastric cancer cells and the underlying molecular mechanisms have not been well elucidated. ***Methods:*** We evaluated PepE effects on gastric cancer cell invasion and migration *in vitro* via wound healing and transwell assays and those on growth and metastasis *in vivo* using an orthotopic xenograft NOD-SCID mouse model. DNA methyltransferase (DNMT) activity was determined using a colorimetric DNMT activity/inhibition assay kit. PepE binding kinetics to DNMTs were determined using the bio-layer interferometry binding assay. Gene and protein levels of DNMTs, AMPKα-Sp1 signaling molecules, and metastatic-suppressor genes in PepE-treated gastric cancer cells were determined using quantitative reverse transcription-PCR arrays and western blotting. The effect of PepE on Sp1 binding to the *DNMT* promoter was determined by electrophoretic mobility-shift assay. Global DNA methylation levels were determined using liquid chromatography coupled with electrospray ionization tandem mass spectrometry. The methylation status of silenced metastatic-suppressor genes (MSGs) in gastric cancer cells was investigated by methylation-specific PCR. ***Results:*** PepE can dose-dependently suppress invasion and migration of poorly-differentiated gastric cancer cells *in vitro* and *in vivo* with low toxicity against normal cells. Mechanistically, PepE not only covalently binds to the catalytic domain of DNMT1 and inhibits its activity (IC_{50} value 3.61 μM) but also down-regulates DNMT1, 3a,

Xin-zhi Wang and Jia-li Gu
School of Pharmacy, Nanjing University of Chinese Medicine; Nanjing University of Science and Technology Hospital, Nanjing University of Science and Technology; Xianlin Avenue No. 138, Nanjing; Xiaolinwei Lane No. 200, Nanjing (China); Tel. +86-025-858 11839, Fax +86-025-858 11839 E-Mail wxzatnj@sina.com; jialigu05@163.com

and 3b mRNA and protein expression in in gastric cancer cells, by disruption of the physical interaction of Sp1 with the *DNMT1*, *3a*, and *3b* promoter and mediation of the AMPKα-Sp1 signaling pathway. The dual inhibition activity of PepE toward DNMTs renders a relative global DNA hypomethylation, which induces MSG promoter hypomethylation (e.g., E-cadherin and TIMP3) and enhances their expression in gastric cancer cells. ***Conclusion:*** Collectively, our data indicated that PepE may represent a promising therapeutic lead compound for intervention in gastric cancer metastasis and may also exhibit potential as a DNA methylation inhibitor for use in epigenetic cancer therapy.

Introduction

Gastric cancer (GC) is the fourth most common malignancy and remains the second leading cause of cancer-related death worldwide [1, 2]. Lacking early detection markers, GC is usually diagnosed in late stages, which, together with a deficit of effective therapeutic strategies, generally results in poor prognosis [1-4]. Although chemotherapy and radiotherapy have been employed to treat GC, invasion and metastasis of cancer cells remains the main cause of GC related death, with a 5-year survival rate below 25% [5]. Therefore, identifying potential targets for attenuating the metastasis and developing potent therapeutic drugs are critical for effective GC treatment.

Traditional Chinese medicine (TCM) has been widely used to prolong the survival of patients with advanced GC and has become a popular complementary and alternative option for the treatment of malignant tumors owing to its demonstrated therapeutic efficacy and low side effects [6-10]. In particular, natural compounds derived from TCM show considerable promise in devising new chemotherapy drugs for use in patients with GC [10-11]. Nevertheless, the detailed mechanisms by which TCM (or natural compounds derived therefrom) influences GC cell growth and metastasis remain to be elucidated.

Peperomia dindygulensis (Piperaceae) is commonly used in southern China as a complementary medicine to treat advanced/metastatic GC (Chinese name Shi-Chan-Cao) [12]. Chemical analysis of this plant has indicated that it contains various constituents including secolignans [13-14], tetrahydrofuran lignans [15], flavonoids [16], and polyketides [17, 18]. Secolignans are characteristic of the *Peperomia* species and have been shown to possess bioactivities that render them as effective treatments against tumors and inflammation [14, 19, 20]. Peperomin E (PepE) (Fig. 1), a secolignan characterized by an α-methylene-γ-butyrolactone moiety, has shown the strongest inhibition of tumor cell growth ability among the secolignans that have been isolated. Specifically, a previous study indicated that this molecule inhibited cell proliferation and induced apoptosis of GC cells *in vitro* and *in vivo* through mitochondrial and PI3K/Akt signaling pathways with relative safety, and thus has the potential to be used as a lead compound for further development as a chemotherapy agent against GC [21]. However, the effects and detailed mechanism of PepE on the inhibition of metastasis and invasion in GC cells have not yet been examined, as the primary clinical use of *P. dindygulensis* in China has targeted advanced/metastatic GC.

In previous decades, much effort has been made to identify prognostic biomarkers and drug targets in patients with advanced and metastatic GC [4]. As recently reported by multiple clinical studies, tumor cells require genetic and/or epigenetic changes in order to be transformed into metastatic cells [22]. DNA methylation, accomplished by a family of DNA methyltransferase (DNMT) enzymes, plays a critical role in epigenetic gene regulation in many forms of cancer including GC [23-27]. Moreover, the aberrant hypermethylation of a substantial number of metastatic-suppressor genes (MSGs), such as cadherins (i.e., E-cadherin) and tissue inhibitor of metalloproteinases (i.e., TIMP-3), has been widely investigated [28-44]. Increasing evidence has shown that E-cadherin and TIMP-3 are highly frequently methylated in tumor tissues from patients with advanced GC as well as in poorly differentiated GC cells (mainly owing to the overexpression of DNMTs in these cells), but not in adjacent normal tissues or normal cells, and that this, at least in part, leads to gene

silencing [34-44]. It has also been reported that the methylation of these genes is associated with poor prognosis of patients with GC, emphasizing their potential clinical significance [45]. Because restoring E-cadherin and TIMP-3 expression in GC cells decreased tumor migration and invasion, epigenetic interference with these hypermethylated MSGs has been gaining considerable attention as a promising target against GC metastasis [32, 33, 46, 47].

Here, we report for the first time that PepE inhibits the methylation activity of DNMT1 by physically binding to its catalytic domain, and down-regulates DNMT expression through mediation of the AMPKα-Sp1-DNMT signaling pathway. This results in significant DNA hypomethylation and the restoration of the function of the inactivated MSGs, E-cadherin and TIMP3, which interfere with the growth, invasion and metastasis of poorly differentiated GC cells *in vitro* and *in vivo*.

Materials and Methods

Reagents and cell culture

PepE was previously isolated in our laboratory via a series of chromatographic procedures from the whole plant of *P. dindygulensis*, which was collected from Yunnan province, China in February, 2014. Its structure was unequivocally elucidated using multiple spectroscopic methods (Fig. S1 - for all supplemental material see www.karger.com/10.1159/000495096/). The purity of PepE was verified by high performance liquid chromatography peak area normalization and peak purity analysis. Results showed that the purity was >98% and the peak purity angle/peak purity threshold was <1 (Fig. S2).

PepE was dissolved in dimethylsulfoxide (DMSO) (Sigma Aldrich, St. Louis, MO, USA) to produce a 10^{-2} M stock solution. Decitabine (5-Aza-dC, CAS No. 2353-33-5), bortezomib (CAS No. 179324-69-7), and dorsomorphin dihydrochloride (CAS No. 1219168-18-9) were all purchased from Abmole Bioscience Inc. (Houston, TX, USA) and dissolved in DMSO immediately prior to use. 5-methyl-2-deoxycytidine (5mdC), 2-deoxycytidine (2dC), and 2-deoxyguanosine (2dG) were obtained from Sigma Aldrich. D-luciferin phosphate (CAS No. 145613-12-3) were purchased from Santa Cruz Biotechnology (Santa Cruz, CA, USA). Human DNA (Cytosine-5) methyltransferase enzyme 1 (DNMT1, 250 Units) was purchased from New England Biolabs (Ipswich, MA, USA). Human DNA (Cytosine-5) methyltransferase enzyme 3a (DNMT3a, 10 μg) and mouse DNA (Cytosine-5) methyltransferase enzyme 3b (DNMT3b, 10 μg) were purchased from Epigentek (Farmingdale, NY, USA).

The antibodies against DNMT1, DNMT3a, DNMT3b, E-cadherin, TIMP3, metalloproteinase (MMP)-2, MMP-9, and Sp1 were all purchased from Abcam (San Francisco, CA, USA). Monoclonal antibodies specific for AMPKα and its phosphor-forms were purchased from Cell Signaling Technology Inc. (Beverly, MA, USA). Sp1, DNMT1 and negative control small interfering RNAs (siRNAs), GAPDH, and horse radish peroxidase (HRP)-conjugated secondary antibodies (goat anti-rabbit) were obtained from Santa Cruz Biotechnology. Gibco fetal bovine serum (FBS) and RPMI-1640 media were purchased from Thermo-Fisher Scientific (Rockford, IL, USA).

The poorly differentiated GC cell line NCI-N87, MGC-803; undifferentiated GC cell line HGC-27 and human gastric mucosal epithelial cell line GES-1 were all obtained from BeNa Culture Collection Ltd. (Beijing, China). The NCI-N87 cells tagged with luciferase reporter gene (NCI-N87-Luc, Cat. No. CBP30870) were obtained from the Cobioer biotechnology Inc. (Nanjing, Jiangsu, China). All the tested cells were passaged in our laboratory for < 6 months after resuscitation, cultured and maintained in 90% (v/v) RPMI-1640 supplemented with 10% (v/v) FBS, 100 U/mL penicillin, and 100 μg/mL streptomycin, and grown at 37 °C in a 5% CO_2 humidified incubator.

Proliferation assay

The effects of PepE on GC cell viability were investigated using MTT assays. Briefly, cells were counted and seeded into a 96-well microtiter plate (4 x 10^3 cells/well). The cells were treated with increasing concentrations of PepE for up to 48 h, followed by adding 20 μL MTT solution (5 mg/mL in phosphate buffered saline (PBS)) at incubating at 37 °C for an additional 4 h. The supernatant was removed, then 150

μL DMSO was added to each well and oscillated for 10 min. Absorbance at 490 nm was determined using a 96-well Multiskan Go microplate reader (Thermo-Fisher Scientific). Inhibition ratio (%) was calculated as [absorbance of control – absorbance of test sample)/absorbance of control] x 100%.

Wound healing assay

GC cells were seeded into 12-well plates at a density of 5 x 10^5 /well. After 24 h, confluent monolayers were scratched with a 1 mL plastic pipet tip to create a uniform, cell-free area. Then, the cells in each well were incubated with serum free RPMI-1640 medium and treated with or without PepE at concentrations of 0.5, 1.0, and 2.0 μM for 24 h. Cells were photographed at time points 0 and 24 h using an Olympus CKX 41 inverted microscope (Tokyo, Japan). Digital images were acquired with a DP22 digital camera (Olympus) and the migrated cells to the denuded zone in microscopic fields (X 100) were counted and the mean count was calculated according to previously reported [48].

Transwell migration and invasion assay

Cell migration and invasion were detected using Transwell chambers (Corning, Armonk, NY, USA) with a pore size of 8.0 μm in diameter. For the cell migration assay, the lower chamber was filled with 600 μL RPMI-1640 medium supplemented with 10% FBS, and the upper chamber was supplemented with 100 μL GC cell suspension at 1 x 10^5 cell/mL in RPMI-1640 medium without FBS, instead containing PepE at concentrations of 0, 0.5, 1.0, and 2.0 μM. After incubation at 37 °C for 24 h, the non-migrating cells (cells remaining on the upper side of the Transwell membrane) were carefully cleaned off with cotton swabs and migrating cells (cells accumulating on the lower side of the Transwell membrane) were fixed with 95% (v/v) ethanol for 5 min, and then stained with 5 mg/mL crystal violet for 5 min and observed using a microscope (X 200). Cells in six random microscopic fields were counted and the mean count was calculated.

For the cell invasion assay, the upper chamber was coated with 100 μL of 1:8 diluted Matrigel gel (BD Biosciences, San Jose, CA, USA). The lower chamber was filled with RPMI-1640 medium supplemented with 10% FBS. After the gel in the upper chamber was solidified, 200 μL GC cells (1 x 10^5 cells/mL) in RPMI-1640 medium containing PepE at concentrations of 0, 0.5, 1.0, and 2.0 μM was added to the upper chamber. After incubation at 37 °C for 48 h, the cells remaining in the upper chamber together with the gel were cleaned off carefully with cotton swabs and the invasive cells (cells accumulating on the lower side of the Transwell membrane) were fixed with 95% (v/v) ethanol for 5 min, and then stained with 5 mg/mL crystal violet for 5 min. Cells in six random microscopic fields (X 200) were counted and the mean count was calculated.

DNMT activity assay

Nuclear extracts were prepared from NCI-N87, MGC-803, and HGC-27 cells using the Epiquik nuclear extraction kit (Epigentek) following the manufacturer's instructions and stored at −80 °C. The DNMT activity was determined using an Epiquik DNMT activity/inhibition assay kit (Colorimetric, Epigentek) following the manufacturer's instructions. Briefly, 10 μg nuclear extracts or 20 ng recombinant DNMT1, 3a, or 3b enzyme (purchased from New England Biolabs) was added to the sample wells coated with cytosine-rich DNA substrate. Then, different concentrations of PepE or 5-Aza-dC were added to the wells, with control wells receiving DMSO only. The substrate reaction was read spetro-photometrically at 450 nm using a 96-well microplate reader. Inhibition rates were calculated using the following formula, IC_{50} was calculated from the dose-inhibition curves.

$$\text{Percent activity (\%)} = \frac{Inhibitor\ Sample\ OD - Blank\ OD \quad Inhibitor\ Sample\ OD - Blank\ OD}{No\ Inhibitor\ Sample\ OD - Blank\ ODNo\ Inhibitor\ Sample\ OD - Blank\ OD}$$

Molecular modeling

The three-dimensional (3D) structure of DNMT1 was obtained from the Protein Data Bank (PDB ID: 4WXX), comprising an X-ray structure with a 2.62 Å resolution of DNMT1 in complex with S-adenosyl-L-homocysteine (SAH). The protein was prepared for docking by using the Protein Preparation Wizard in Discovery Studio version 4.0 (DS 4.0, Accelrys, San Diego, CA, USA). All crystallographic water molecules were deleted and a 15 radius grid (XYZ coordinates: −47.481, 61.396, 6.933) binding site was generated based on the previously reported catalytic domain of this protein. PepE was prepared using the Prepare Ligands module of DS 4.0 under the MMFF94x force field and a specifying pH value of 7.0. Several standard

procedures of DS CDOCKER docking protocols were performed. These docking procedures allowed ligand docking flexibility and a total of 10 top ranked structures were analyzed for studying receptor-ligand interactions between PepE and DNMT1.

Bio-layer Interferometry (BLI) binding assay

The binding kinetics of PepE to recombinant active human DNMT1 were determined using BLI on an Octet RED 96 system (ForteBio, Shanghai, China) following manufacturer protocol. All interaction analyses were performed at 25 °C in PBS plus 0.2% DMSO buffer. Purified recombinant DNMT1 was pre-labeled with biotin using a streptavidin (SA) conjugation kit (Abcam) according to manufacturer instruction. Loading of Dip and Read™ Streptavidin Biosensors (ForteBio) was conducted by exposing biotinylated DNMT1 (0.01 mg/mL) to biosensor tips for 2 h. The 96-well microplates used in the Octet were filled with 200 μL of sample or buffer per well and agitated at 1000 rpm. The loaded biosensors were washed in buffer for 600 s and transferred to wells containing PepE, 5-Aza-dC, and Peperomin A (PepA, secolignan isolated from *Peperomia dindygulensis*, which shares the same skeleton of PepE, except the α-methylene-γ-butyrolactone moiety is replaced by an α-methyl-γ-butyrolactone moiety)[14] at concentrations of 12.5, 25, 50, 100, and 200 μM in buffer, respectively. The association and dissociation was observed for 90 s for each sample diluent. Reference measurements were conducted by using buffer instead of PepE. A parallel set of SA unloaded biosensors was prepared to act as a control. The sample-sensorgrams were corrected by subtracting the double reference curve. Kinetic parameters (K*on* and K*off*) and affinity (K_D) were determined from a global fit to a 1:1 binding model of the data between DNMT1 and PepE, PepA, or 5-Aza-dC using Octet software (ForteBio).

Quantitative real-time reverse transcription-PCR assay

RNA was extracted from GC cells using the RNeasy RNA isolation kit (Qiagen, Hilden, Germany), and on-column DNA-digestion was performed using the RNase-free DNase Set (Qiagen). RNA (2 μg) was reverse transcribed using the iScript cDNA synthesis kit (Bio-Rad, Hercules, CA, USA) according to the manufacturer's protocol, and gene expression levels of DNMT1, DNMT3a, DNMT3b, E-cadherin, and TIMP3 were quantitatively measured in triplicate using a real-time quantitative PCR system (QuantStudio 3 Real-Time PCR, Thermo-Fisher Scientific), using SYBR Green I (Applied Biosystems) and corresponding primers (Table S1, designed by the software Primer premier 5.0 and synthesized by Genewiz Corp., Suzhou, China). The PCR conditions are listed in Table S2. The mRNA levels of all tested genes were normalized against *GAPDH*, results are reported as fold change ($2^{-\Delta\Delta CT}$) relative to non-treated samples.

Methylation-specific PCR assay

Methylation-specific PCR was performed based on a previously described method. Briefly, DNA was extracted from PepE (0, 0.5, 1, and 2 μM) or 5-Aza-dC (2 μM)-treated GC cells using the DNeasy tissue kit (Qiagen) according to the manufacturer's instructions. Extracted DNA (1 μg) was modified with bisulfite using a CpGenome DNA modification Kit (Chemicon, Temecula, CA, USA). The modified DNA was amplified with primers for the methylated and unmethylated genes designed according to previously published reports (Table S3). The reactions were carried out using the Veriti 96 well thermal cycler (Applied Biosystems). The PCR conditions are listed in Table S4. The PCR products were then loaded onto 3.5% low range agarose gels (Thermo-Fisher Scientific), stained with ethidium bromide, and observed under UV illumination using a Gel Doc XR Gel Documentation system (Bio-Rad).

Western blot analysis

The western blot was performed based on our previous studies. In brief, the lysates from the cultured GC cells (approximately 50 μg proteins) were separated on 10% sodium dodecyl sulfate polyacrylamide gels. Membranes (Abcam) were incubated with antibodies against DNMT1, DNMT3a, DNMT3b, E-cadherin, TIMP3, MMP-2, MMP-9, Sp1, AMPKα, p-AMPKα (Thr 172), and GAPDH (1:1000). The membranes were washed and incubated with the HRP-conjugated secondary antibodies. Subsequently, the membranes were transferred to freshly made ECL solution (Millipore, Waltham, MA, USA), followed by observing and documenting the signals under the Gel Doc XR Gel Documentation system (Bio-rad). Grey-levels were analyzed using Gel-pro 32 software (Media Cybernetics, Rockville, MD, USA) with normalization to GAPDH. Experiments were repeated three times.

Electrophoretic mobility-shift assay (EMSA)

EMSA was performed as previously described [49-51]. Briefly, oligonucleotide probes including *DNMT1*, *DNMT3a* (3A-P3-W1, DNMT3a 3rd promoter), and *DNMT3b* (3B-P1-W1, DNMT3b 1st promoter) promoter regions that contain putative Sp1-binding sites were chemically synthesized, and complementary oligos were annealed and labeled with ^{32}P-dCTP by Klenow fragment (Life Technologies, Carlsbad, SA, USA; the oligo sequences used in this study are previously reported by Liu et al. [49, 50] and Jinawath et al. [51]). Nuclear extracts were prepared using an Epiquik nuclear extraction kit (Epigentek). EMSA with nuclear extracts and ^{32}P-labeled *DNMT1*, *DNMT3a*, and *DNMT3b* promoter oligos was performed as previously described [49-51]. For antibody super-shift assays, 4 μg Sp1 antibody or control rabbit IgG (Cell Signaling Technology, Mountain View, CA, USA) was added after the binding reactions proceeded 20 min, and further incubated for another 30 min before gel loading. Alternatively, nuclear extracts were pre-incubated with Sp1 antibody at 4 °C for 24 h before being added to the binding reactions.

Global DNA methylation analysis

NCI-N87, MGC-803, and HGC-27 cells were treated with PepE at concentrations of 0, 0.5, 1, 2, or 4 μM or with 5-Aza-dC (1 μM) for 48 h. Genomic DNA was isolated and purified from the treated GC cells and tumor tissues extracted from the orthotopical *in vivo* studies (50mg/kg/d) using the DNeasy tissue kit (Qiagen, Valencia, CA, USA) following manufacturer instruction and stored at −80 °C. Global methylation levels were determined by liquid chromatography coupled with electrospray ionization tandem mass spectrometry as described previously by Song et al. [52]. Briefly, 0.5 μg genomic DNA was hydrolyzed to single nucleotides using the Epiquik one-step DNA hydrolysis kit (Epigentek, Farmingdale, NY, USA) following manufacturer instruction. Digested DNA was separated on a Prominence ultra-fast liquid chromatography system (Shimadzu, Kyoto, Japan) and determined on a triple quadrupole linear ion trap mass spectrometer equipped with a TurboIonSpray ion source (5500 Q-Trap, Applied Biosystems, Foster City, CA, USA). Quantification was undertaken in multiple reaction monitoring (MRM) mode by monitoring transition pairs as described by Song et al. [52]. Genomic DNA methylation was expressed as [5mdC]/[dG]%, which was quantified by using a calibration curve between the peak area ration of 5mdC to dG (A_{5mdC}/A_{dG}) versus [5mdC]/[dG]%.

Treatment with small interfering RNAs (siRNA)

NCI-N87 cells were seeded in six-well culture plates in RPMI-1640 medium containing 5% FBS, and grown to 70% confluence prior to incubation with SiRNAs, Sp1 SiRNAs (No. sc-29487, Santa Cruz Biotechnology), DNMT1 SiRNAs (No. sc-35204, Santa Cruz Biotechnology) or control of SiRNA oligonucleotides (No. sc-37007, Santa Cruz Biotechnology) were transfected using the siRNA transfection reagent (No. sc-29528, Santa Cruz Biotechnology) according to the manufacturer's instructions and incubated with MEM medium (Gibco) for 30 min at room temperature before the mixture was added to the cells. After culturing for up to 30 h, the cells were washed and re-suspended in fresh medium for an additional 24 h for further experiment. RNAs and proteins from transfected NCI-N87 were extracted for further analysis.

Animal studies

Six-week-old female BALB/c athymic nude mice and NOD-SCID mice (obtained from the model animal research center of Nanjing University, Nanjing, China) were acclimated for 1 week and caged in groups of five. All animal studies were conducted under guidelines approved by the Animal Care and Use Committee of the Nanjing University of Chinese Medicine (Nanjing, China).

To investigate the antitumor effects of PepE, NCI-N87 cells ($2x10^6$; 0.2 ml) were injected subcutaneously into the dorsal area of the BALB/c athymic nude mice. After 7 days, when tumors reached 5 mm in diameter, the mice were randomly assigned to two groups: (a) daily intra-gastric (i.g.) dose of soybean oil (control group, n = 5); and (b) daily i.g. 50 mg/kg of PepE (dissolved in soybean oil, n = 5). Mice were treated for 3 weeks. At the end of the treatment period, all mice were sacrificed, their tumor tissues were excised, weighed and placed in either 10% buffered formalin for paraffin fixation or frozen in liquid nitrogen for further observations.

To investigate the anti-metastatic activity of PepE *in vivo*, NCI-N87 cells tagged with luciferase reporter gene (NCI-N87-Luc) were orthotopic transplanted into the stomach of NOD-SCID mice according to previous reported methods [53, 54]. 6 days after transplantation, mice with NCI-N87-Luc tumor implants were subjected to bioluminescent analysis based on the luciferase signal. Briefly, mice were received

D-luciferin phosphate solution (100 mg/kg) intravenously at 10 min prior to imaging, then anesthetized with isofluorane by inhalation and imaged by a Xenogen IVIS scanner (PerkinElmer, Waltham, MA, USA). The next day, mice showing successful implantation of tumor were randomly divided into the control group (n = 5) and treatment group (n=5), which daily i.g. of soybean oil and PepE (50 mg/kg), respectively. Growth and local metastasis of NCI-N87-Luc cells of mice were then monitored at 21 and 35 days by their luciferase light signal. 35 days after the tumor transplantation, all mice were sacrificed and their livers, spleens and kidneys were excised for *ex vivo* bioluminescent imaging to determine the metastasis of NCI-N87-Luc cells to other organs. The above bioluminescent signal intensity was all quantified using the Living Image software (version 4.2, Carliper Life Science, Inc., Hopkinton, MA, USA) and presented as the photons/second/cm^2/sr (sr denotes steradian).

Immunohistochemical observation

The tumor excised from *in vivo* experiment were fixed in 10% neutral formalin, embedded in paraffin, and cut into 4-μm thick sections. The tumor tissue sections were incubated in 3% hydrogen peroxide for 15 min and then in normal goat serum for 20 min to block endogenous peroxidase activity and nonspecific binding sites. Sections were incubated for 4 h with antibodies against DNMT1, DNMT3a, DNMT3b, E-cadherin, and TIMP3 (1:100 dilution), then treated with biotinylated secondary antibodies (1:200 dilution), and antibody-binding sites were visualized by 3, 3'-diaminobenzidine staining (Dako, Carpinteria, CA, USA). Sections were observed under an Olympus CKX 41 inverted microscope.

Statistical analysis

Statistical analyses were undertaken using GraphPad Prism 6.0 software (GraphPad Software Inc., La Jolla, CA, USA). One-way ANOVA followed by Student's t-test was used for multiple comparison. $P < 0.05$ was considered significant and $P < 0.01$ was considered more significant.

Results

PepE inhibits proliferation, migration, and invasion of GC cells in vitro and in vivo

As we reported previously, PepE can inhibit cell proliferation and induce apoptosis of GC cells [21]. In the present study, we chose GC cell lines with reported metastatic abilities including the poorly differentiated cell line NCI-N87, MGC-803 and undifferentiated cell line HGC-27, to investigate the effects of PepE on proliferation, migration, and invasion abilities and correlated molecular mechanisms in these cells.

As depicted in Fig. 1A, the inhibitory effect of PepE on NCI-N87, MGC-803, and HGC-27 was dose-dependent, with IC_{50} calculated as follows: NCI-N87, 1.3 μM; MGC-803, 1.9 μM, and HGC-27, 2.7 μM. Selectivity for tumor versus normal cells was determined by comparing the efficacy of PepE on the above cancer cells to its efficacy on the normal gastric epithelial cell line GES-1. PepE inhibitory effect on GES-1 was far less potent than that on the tumor cells (IC_{50} value 76.1 μM), indicating that PepE is specific for cancer cells. An *in vivo* subcutaneously implantation of NCI-N87 cells in nude mice was used to examine the inhibiting effects of PepE on *in vivo* inhibition of GC cells. As shown in Fig. 1B, by i.g. administration of PepE at 50 mg/kg/d from day 7 after transplantation of NCI-N87 cells, tumor growth was significantly inhibited in PepE-treated group ($P < 0.01$). The inhibition rate was 60.3% after 3 weeks treatment.

Next, we investigated the effects of PepE on the migration of GC cells by means of a wound closure assay. As shown in Fig. 2A, relative wound closure was higher in control cells when compared with PepE-treated cells. Inhibition was observed when GC cells were incubated with PepE at different doses for 24 h treatment. Quantification analysis of cells migrated to the denuded zone demonstrated that the GC cell migration was significantly reduced in a dose-dependent manner, with migration ability reduced by 63.8%, 37.2%, and 15.9 % in NCI-N87 cells; 78.3%, 53.4% and 11.2% in MGC-803 cells; and 58.7%, 24.3%, and 9.4% in HGC-27 cells, as compared to the control group, when cells was incubated with 0.5, 1.0, and 2.0 μM PepE, respectively.

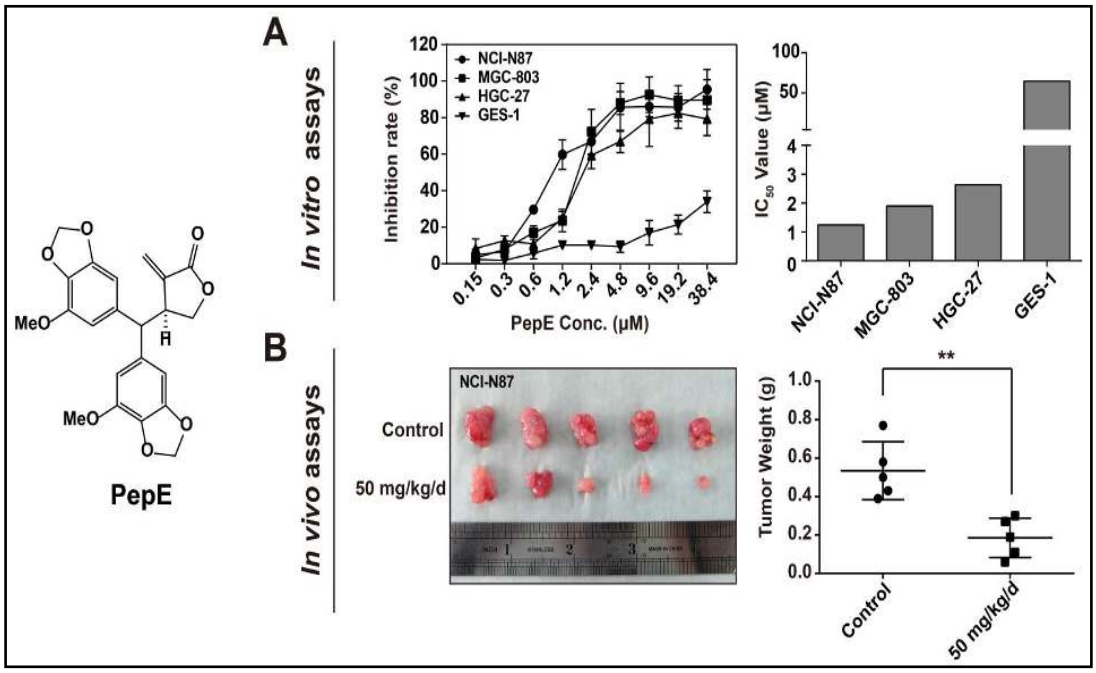

Fig. 1. In vitro and in vivo antitumor activity of PepE against poor differentiated GC cells. (A) growth inhibition rates of gastric mucosal epithelial cell line GES-1 and GC cell lines treated with PepE at the indicated concentrations for 48 h. Data shown are means ± SD (n=3). (B) anticancer effects of PepE in the NCI-N87 nude mice model, NCI-N87 cells were subcutaneously implanted into the dorsal area of BALB/C athymic nude mice and PepE therapy were begun on day 7. Administration of 50 mg/kg/d PepE were effective at inhibiting tumor growth after 3 weeks of therapy (**P<0.01 when compared with control).

To further confirm whether PepE inhibited the migration of GC cells, Transwell chamber experiments were used. As shown in Fig. 2B, PepE inhibited the migration ability of GC cells in a concentration-dependent manner. Quantification analysis indicated that migration ability reduced by 68.7%, 23.1%, and 18.1% in NCI-N87 cells; 61.3%, 37.1%, and 18.7% in MGC-803 cells; and 62.3%, 38.4%, and 31.2% in HGC-27 cells, as compared to the control group, when cells were incubated with 0.5, 1.0, and 2.0 μM PepE, respectively.

The effect of PepE on the invasion of GC cells was examined using Matrigel invasion chambers. As shown in Fig. 2B, compared to the untreated control, the number of invading cells represented by crystal-violet stain was markedly reduced in a dose-dependent manner in GC cells. Quantification analysis indicated that the inhibitory effects on cancer cell invasion, as measured by the percentage of control, were 62.5%, 27.1%, and 18.1% in NCI-N87 cells, 68.3%, 23.1%, and 17.9% in MGC-803 cells, and 62.7%, 28.9%, and 11.9% in HGC-27 cells, when treated with 0.5, 1.0, and 2.0 μM PepE, respectively.

Since PepE strongly attenuated migration and invasion of GC cells *in vitro*, we next examined the effect of PepE on metastasis of NCI-N87 cells in NOD-SCID mice xenograft model. To do this, we applied NCI-N87-Luc cells, which stably expresses constitutive luciferase and enable tumor growth and metastasis to be monitored by bioluminescent imaging. According to Fig. 3A, the luciferase light signal was detected 6 days after NCI-N87-Luc cell transplantation and the signal was mainly focus on the stomach region. The next day, mice were assigned to receive PepE treatment (50mg/kg) or soybean oil daily. According to Fig. 3A and 3B, tumor implants in the control group continued to grow and invade to other organs, giving out very strong bioluminescence signals after 35 days of tumor transplantation. In contrast, the PepE-treated group has no remarkable enhancement of luciferase signal. The signal intensity, as shown in Fig. 3A and 3B, was significantly weaker when compared to the control group (P<0.05 at 21 days and P<0.01 at 35 days of transplantation). This indicates that in the presence of PepE, the growth and metastasis of NCI-N87-Luc cells were significantly

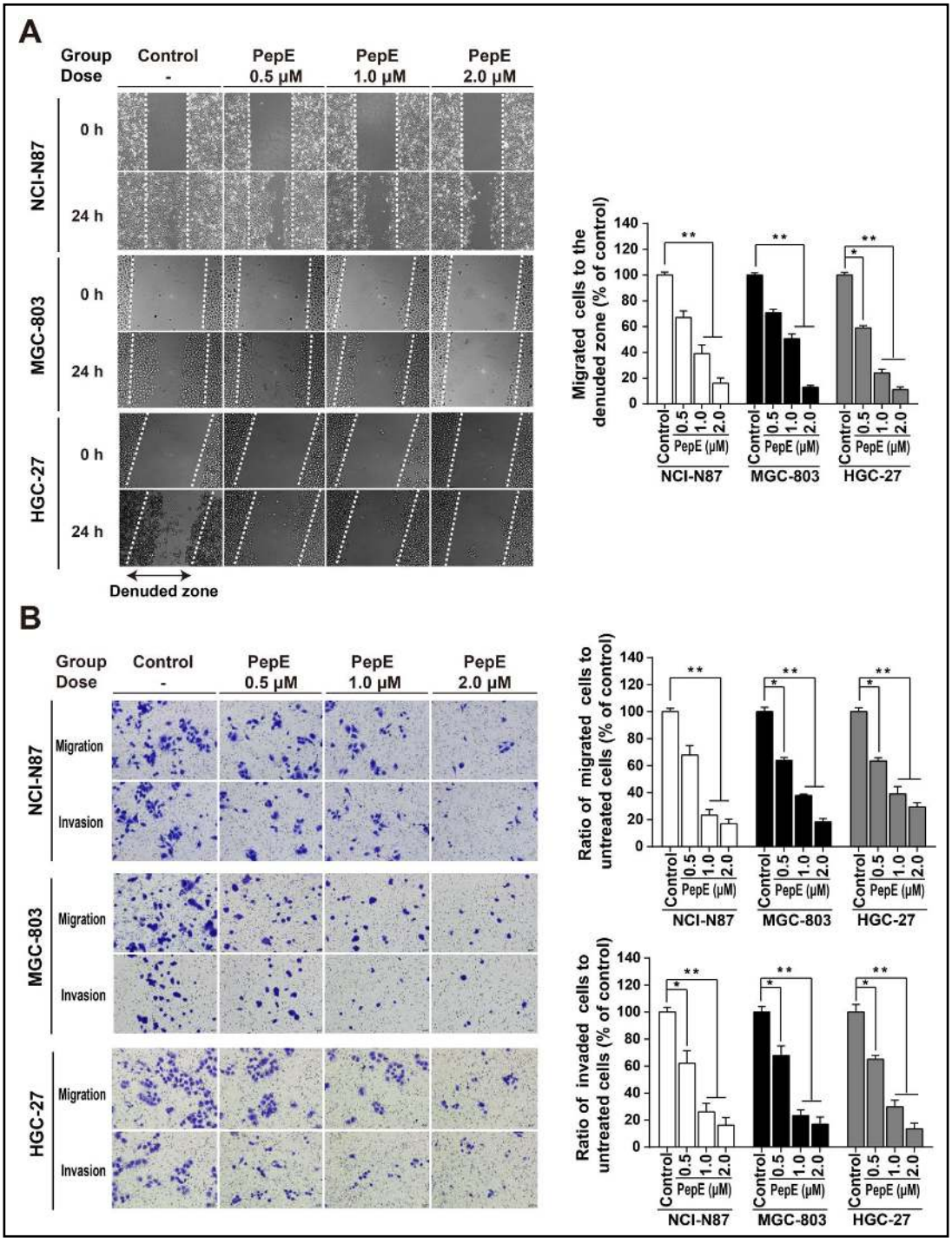

Fig. 2. Effects of PepE on migration, invasion ability in poor differentiated GC cells. (A) Wound healing assay with GC cells. Microscopic observations were recorded 0 and 24 h after scratching the cell surface (100x). Representative images are shown (By left). Histograms (By right) showed the ratio of migrated cells to the denuded zone of PepE treated cells when compared with control. *P<0.05; **P<0.01. (B) Representative images of migrated/invaded GC cells through chambers' membrane (200x, By the left). Histograms showed the ratio of migration cells and invasion cells in PepE treated group when compared with control (By the Right). Cell numbers were counted in five randomly selected microscopic fields (*P<0.05; **P<0.01). All the above data is shown as mean ± SD of three independent experiments.

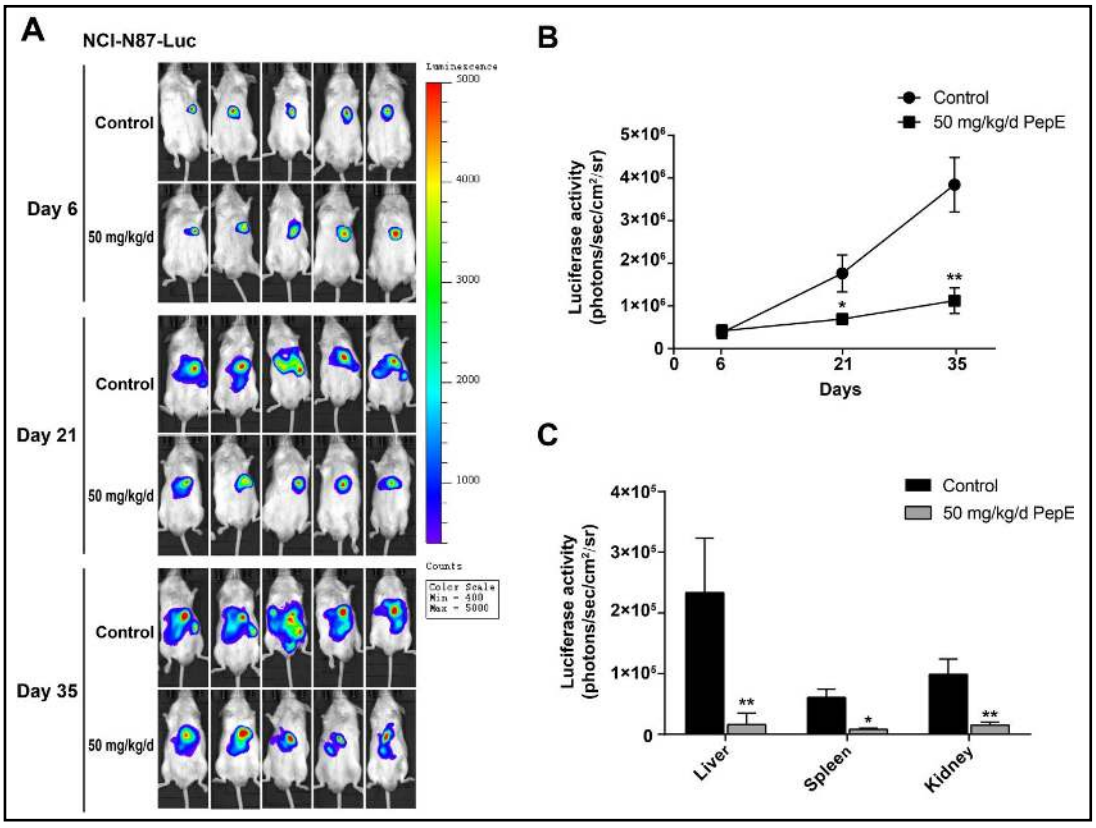

Fig. 3. Therapeutic efficacy of PepE on suppressing the primary and metastatic growth of NCI-N87 cells in orthotopic NOD-SCID mice model. NCI-N87 cells tagged with luciferase reporter gene were orthotopically implanted in to the dorsal side of NOD-SCID mice. (A) Luciferase signal was followed at day 6, 21 and 35 by injecting D-luciferin phosphate into the mice and visualized under bioluminescence imager. Mice were i.g. administrated with PepE (50 mg/kg) or soybean oil (as control) daily. The color scale indicates the signal intensity, which is directly proportional to the number of NCI-N87 cells. (B) Quantitative analysis of the growth and metastatic of NCI-N87 cells by measurements of luciferase activity in mice treated with soybean oil (control) and PepE at day 6, 21 and 40, respectively. (C) At day 35, livers, spleens and kidneys from both control and PepE-treated mice were excised and imaged, the bioluminescence signals of excised livers, spleens and kidneys were quantified for each group of mice. All data are presented as mean ± SD (n=5). *P<0.05, **P <0.01 when compared with control.

inhibited *in vivo*. At the end of the experiment, all mice were euthanized, organs including liver, spleen and kidney were carefully excised and imaged. The overall luciferase signal in the liver, spleen and kidney, representing the extent of metastasized NCI-N87-Luc cells, was found much stronger in control group than in PepE-treated group ($P<0.05$ in spleens, $P<0.01$ in livers and kidneys). This finding ensured that PepE treatment was effective in inhibiting the NCI-N87-Luc cells invade to the liver, spleen and kidney organs in orthotopic mice model.

PepE directly binds and inhibits DNMT1 activity

Transcriptional silencing of metastatic suppressor genes (MSGs) including E-cadherin and *TIMP3* by DNA promoter hypermethylation plays a crucial role in the metastasis of advanced GC [38, 44]. This aberrant methylation is mainly attributed to the abnormal increased expression and activity of DNMTs, including DNMT1, DNMT3a, and DNMT3b in advanced/metastatic GC cells, which catalyze the transfer of methyl groups from S-adenosylmethionine to cytosines in CpG dinucleotides [22, 23, 25]. Therefore, DNMTs have been considered by researchers as promising therapeutic targets in treating the metastasis of advanced GC.

As we reported previously, we found that PepE suppressed DNMT activity in a dose-dependent manner in A549 non-small lung cancer cells [55], and we further confirmed this effect in poorly-differentiated GC cells. As depicted in Fig. 4A, we determined DNMT activity in the nuclear extract of NCI-N87, MGC-803, and HGC-27 cells after treatment with various concentrations of PepE. It was found that PepE inhibited DNMT activity in the GC cell extracts in a dose dependent manner, with IC_{50} values of 2.44, 4.50, and 4.90 μM, respectively. To determine whether PepE could inhibit DNMT activity including DNMT1, DNMT3a, and DNMT3b in a cell free system, active recombinant DNMT1, DNMT3a, DNMT3b were added to the sample wells of the Epiquik DNMT activity/inhibition assay kit and treated with various concentrations of PepE, PepA (negative control) and 5-Aza-dC (positive control). Strikingly, as shown in Fig. 4B-F, we found a pronounced selectivity of PepE toward DNMT1 in the tested compound range with IC_{50} value of 3.61 μM (the IC_{50} value of 5-Aza-dC positive control against DNMT1 was determined as 1.08 μM, the IC_{50} value of PepA negative control against DNMT1 was determined as 151.4 μM). Under these conditions, the enzymatic activity of DNMT3a and DNMT3b were slightly (IC_{50} value of 96.3 μM against DNMT3a) or even not impacted by PepE.

To determine whether PepE could combine with DNMT1, we docked it in silico to the catalytic domain of DNMT1 (PDB ID: 4WXX, in complex with SAH) using the CDOCKER protocol in DS 4.0 as reported previously. Fig. 5A-C shows 3D and 2D representations of the optimized docked model of PepE with the catalytic site of DNMT1. Figure 5d shows the simulated bindings of PepE and the cofactor SAH onto the catalytic site of DNMT1. According to this binding model, the key binding site residues on DNMT1 included those that are within 5-Å reach of the bound PepE molecule (i.e., Cys 1148, Gly 1149, ASN 1578, Pro 1225, Cys 1226, Gln 1575, Glu 1168, Ser 1146, Asn 1578, and Ala 1579). Of these residues, eight are predicted to form H-bonds with PepE, including Cys 1148, Gly 1149, Asn 1578, Pro 1225, Gln 1575, Glu 1168, Ser 1146, and Asn 1578. In addition, the benzene rings of PepE form π-π stacking interactions with Asn 1578 and Ala 1579 of the DNMT1 catalytic site, which binds with DNMT1 in a similar manner as the aminopurine ring of SAH. Moreover, the *α*-methylene-*γ*-lactone moiety of PepE overlaps with the C-5 atom of the cytosine ring in the catalytic space. As the distance between the γ-C atom of the PepE and the C-5 of cytosine is only 1.3 Å, and these atoms are 5.3 and 4.3 Å away from the sulfhydryl group of the catalytic cysteine (Cys 1226), respectively, this model clearly indicated that PepE has the potential to inhibit the DNMT1 catalytic function through its α-methylene-γ-lactone by binding with its Cys 1226 through Michael-type addition. Notably, this is similar to that of the same moiety during parthenolide (a principal bioactive sesquiterpene lactone isolated from feverfew) binding with the DNMT1 catalytic domain [54].

We thus explored the affinity binding kinetics of PepE with DNMT1 using BLI. Consistent with the results of the DNMT activity assay, PepE was found to bind directly to the DNMT1 protein in a dose dependent manner, as shown in Fig. 6 and Table 1. The affinity equilibrium constant revealed a high affinity with K_D value of 3.03×10^{-5} M, which showed slightly lower affinity binding compared to 5-Aza-dC ($K_D = 1.52 \times 10^{-5}$ M). Nevertheless, the binding affinity was much lower between PepA (secolignan with an α-methyl-*γ*-lactone moiety instead of the α-methylene-γ-lactone moiety of PepE) and DNMT1 protein when compared with PepE in the tested compound concentration range, with a K_D value only at 3.12×10^{-2} M, which indicated that the α-methylene-γ-lactone moiety is critically important for PepE binding with DNMT1. Taken together, the above data indicate that PepE physically binds to the catalytic pocket of the DNMT1 protein to selectively inhibit DNMT1 activity.

PepE down-regulates DNMT1, 3a, and 3b expression in GC cells in vitro and in vivo

To determine whether PepE affected the protein expression levels of the DNMTs, we treated the above GC cells with different concentrations of PepE (1, 2, and 4 μM) and 0.1 μM of mithramycin (positive control) for 48 h. It was observed that PepE causes a dose-dependent down-regulation in the protein levels of DNMT1, DNMT3a, and DNMT3b in both cell lines (Fig. 7A). The ability of PepE to down-regulate DNMT expression was also evaluated

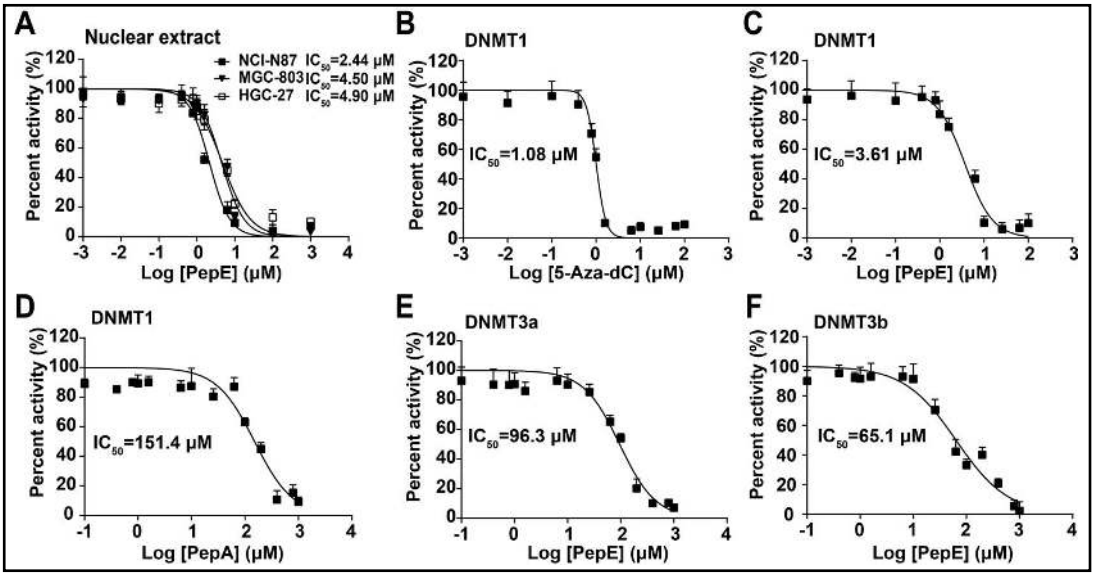

Fig. 4. Dose-response plots for selected compounds (PepE, 5-Aza-dC and PepA) against nuclear extract of GC cells or recombinant DNMTs. The IC_{50} concentrations of selected compounds were determined by colorimetric DNMT activity assays under identical conditions (10 μg nuclear extract or 20 ng recombinant enzyme, 1.6 mM Adomet). Each data point represents the mean ± SD of three measurements, and the data were analyzed by GraphPad Prism version 6.0.

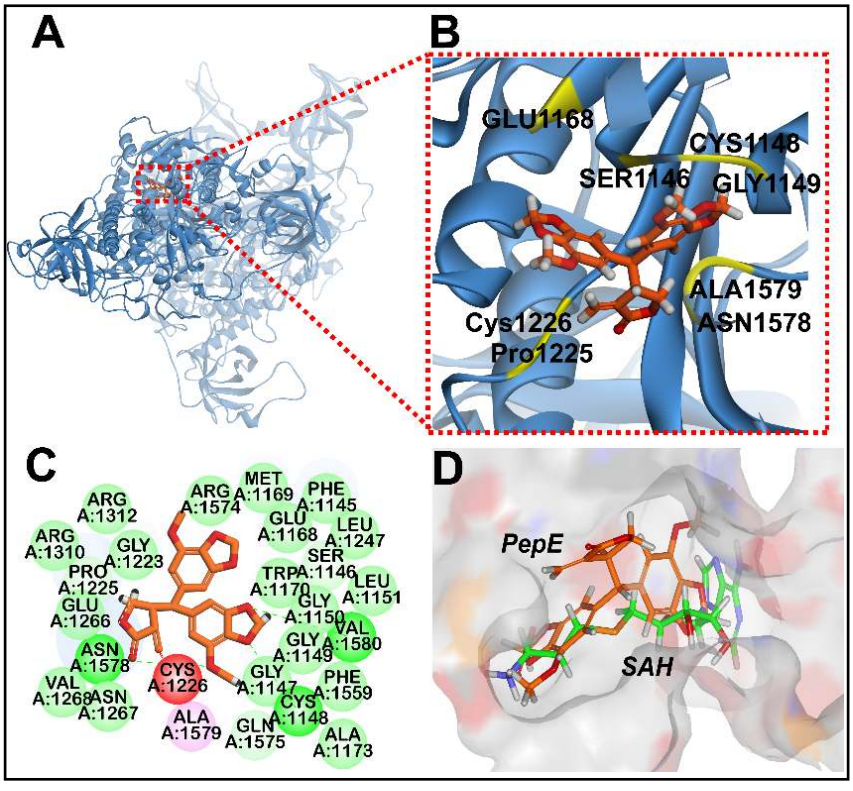

Fig. 5. Molecular modeling of PepE binding to DNMT1. (A) PepE binds to the catalytic domain of DNMT1, (B) indicates an enlarge view. The key binding site residues of PepE on DNMT1 enzyme were marked in yellow, which included those that are within 5-Å reach of the bound PepE molecule. (C) Ligand interaction diagram of the DNMT1 and PepE complex. The colors indicate the residue type (Green: hydrogen bond; Light pink: pi-alkyl, Red: Van der Waals). (D) Superimposed docking of PepE and SAH into the DNMT1 catalytic site and PepE's carbon in orange, SAH carbon in green shown in stick model. DNMT1 active site is represent as a topographic surface is in stick.

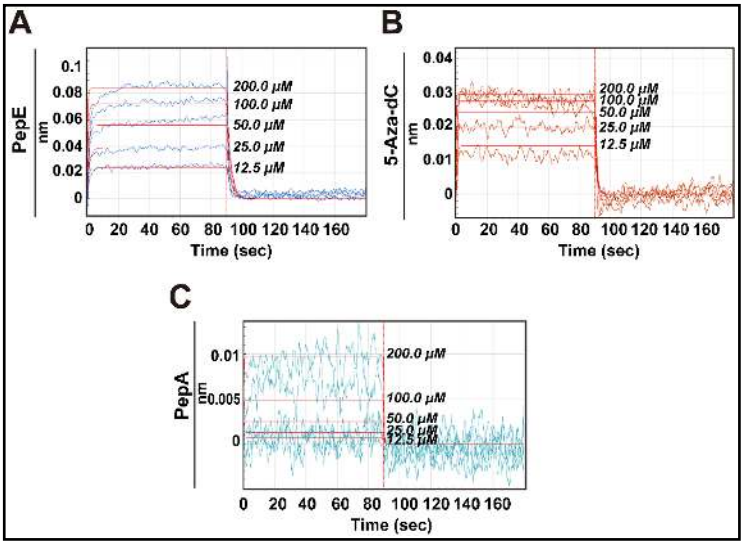

Fig. 6. PepE directly binds to DNMT1 in vitro. Kinetic analysis of the interaction between DNMT1 and PepE (A), 5-Aza-dC (B) and PepA (C) by BLI. The Streptavidin (SA) Biosensor tips coated with SA-tagged DNMT1 were dipped in increasing concentrtions of PepE, 5-Aza-dC and PepA (12.5, 25, 50, 100 and 200 μM) to measure the binding affinity of PepE to DNMT1 (Kon) and subsequently moved to wells containing buffer to measure dissociation rates (Kdis). The affinity constant was calculated as the ratio of the Kdis to the Kon.

in vivo. Immunohistochemical analysis (Fig. 7B) showed that there was a significant decrease in DNMT1, DNMT3a, and DNMT3b levels in the tumor tissue sections of the PepE-treated group when compared to the control group in nude mice model (P<0.01).

Table 1. K_{on}, K_{off} and K_D constants of PepE, 5-Aza-dC and PepA binding with DNMT1

Compounds	K_{on} (1/Ms)	K_{dis} (1/S)	K_D (M)	Full R^2
PepE	9.89×10^{3}	3.10×10^{-1}	3.03×10^{-5}	0.9752
5-Aza-dC	5.82×10^{4}	8.83×10^{-1}	1.52×10^{-5}	0.9494
PepA	1.27×10^{2}	3.96	1.52×10^{-2}	0.8016

Next, we sought to determine whether the observed decline in DNMT1, DNMT3a, and DNMT3b protein levels was due to suppression of their gene expression upon PepE treatment. The mRNA levels of DNMTs were measured by quantitative real-time PCR. It was observed that PepE treatment significantly reduced the mRNA expression of DNMT1, DNMT3a, and DNMT3b, respectively, in a dose dependent manner (Fig. 7C). The above results suggest a specific inhibitory activity of PepE on the expression of DNMT1, DNMT3a, and DNMT3b in tested GC cells both at the gene and protein level.

PepE represses transcription factor Sp1 expression and abrogates its DNA binding activity

Previous studies reported that DNMT1, DNMT3a and DNMT3b gene promoters contain Sp1 transcription factor binding sites, which regulate the expression and function of DNMTs in several cell systems [49, 50, 55, 56]. To support our hypothesis that Sp1 protein mediates DNMT expression in GC cell systems, Sp1 was knocked down using Sp1 SiRNA in NCI-N87 cells. A concurrent decrease in DNMT1, DNMT3a and DNMT3b was observed, thereby supporting the role of Sp1 protein in regulating DNMT expression in GC (Fig. 8A). Next, we tested the changes of Sp1 after PepE treatment. As shown in Fig. 8B, PepE induced a dramatic decrease in Sp1 protein level in a dose-dependent manner in all tested GC cells; additionally, the Sp1 protein level was decreased in bortezomib (positive control, compound that inhibits Sp1 protein function and expression) -treated GC cells [49].

To determine the effect of PepE on the Sp1 binding to the DNMT1, 3a, and 3b promoter, EMSAs were performed with nuclear extracts of NCI-N87 cells treated with PepE (2 μM for 24 h). As shown in Fig. 8C, PepE decreased the Sp1 protein binding to the gene promoters of *DNMT1*, *3a*, and *3b*, whereas obvious alteration of Sp1 DNA binding was also observed in bortezomib-treated [55] cells. Western-blot analysis showed that PepE decreased Sp1 protein expression in the same nuclear extracts (data not shown).

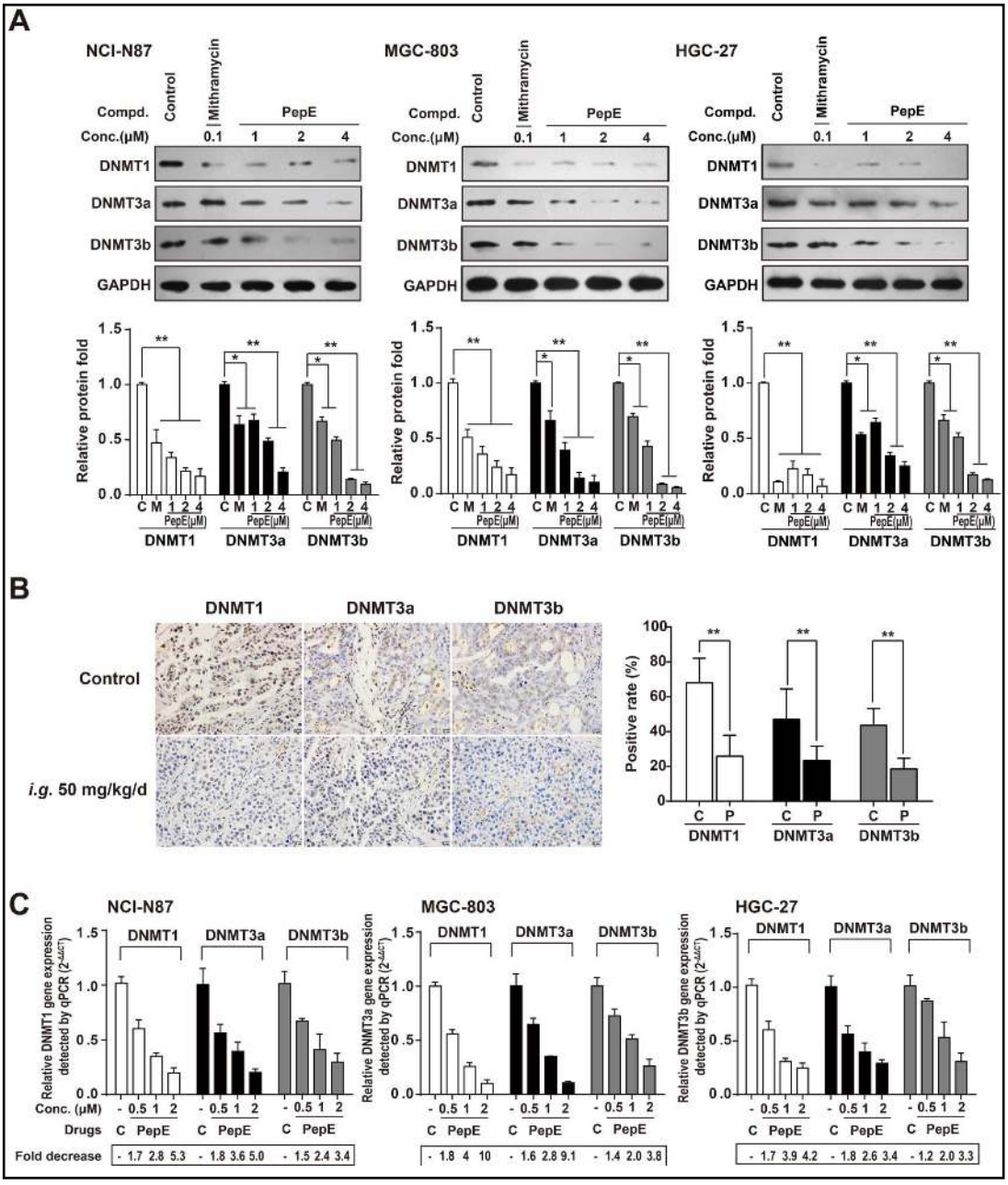

Fig. 7. Effects of PepE on changes of expression of DNMTs in vitro and in vivo. (A) Western-blot bands for DNMT1, 3a and 3b protein expression in NCI-N87, MGC-803 and HGC-27 before and after PepE treatment. The 0.5% DMSO solution and 0.1 μM of mithramycin were used as negative and positive control, respectively. The intensity of the bands was quantified by optical density (OD) and normalized to the OD of GAPDH. Data are presented as mean ± SD (n=3), *P<0.05; **P<0.01. (B) Representative Immunostaining for DNMT1, 3a and 3b in the paraffin section of tumor tissues extracted in NCI-N87 nude mice model. 3 slides per mouse were reviewed. The positive rate was quantified by IOD values and normalized to the IOD values of control (C: control; P:PepE). Data are presented as mean ± SD (n=3), *P<0.05; **P<0.01. (C) DNMT1, 3a and 3b genes' expression in GC cell lines detected by RT-qPCR before and after PepE treatment (C: control). Data are presented as mean ± SD (n=3).

PepE inhibits AMPKα-Sp1-DNMT signaling in GC cells

To further explore the action mechanism of PepE on Sp1 down-regulation, we examined the effect of PepE on the AMPK signaling pathway, which has been recently reported as being involved in mediating the expression of Sp1 [57, 58]. As described in Fig. 8D, PepE produced a significant increase in AMPKα phosphorylation in a dose dependent manner without affecting the level of total AMPKα. We then utilized an AMPK inhibitor to explore

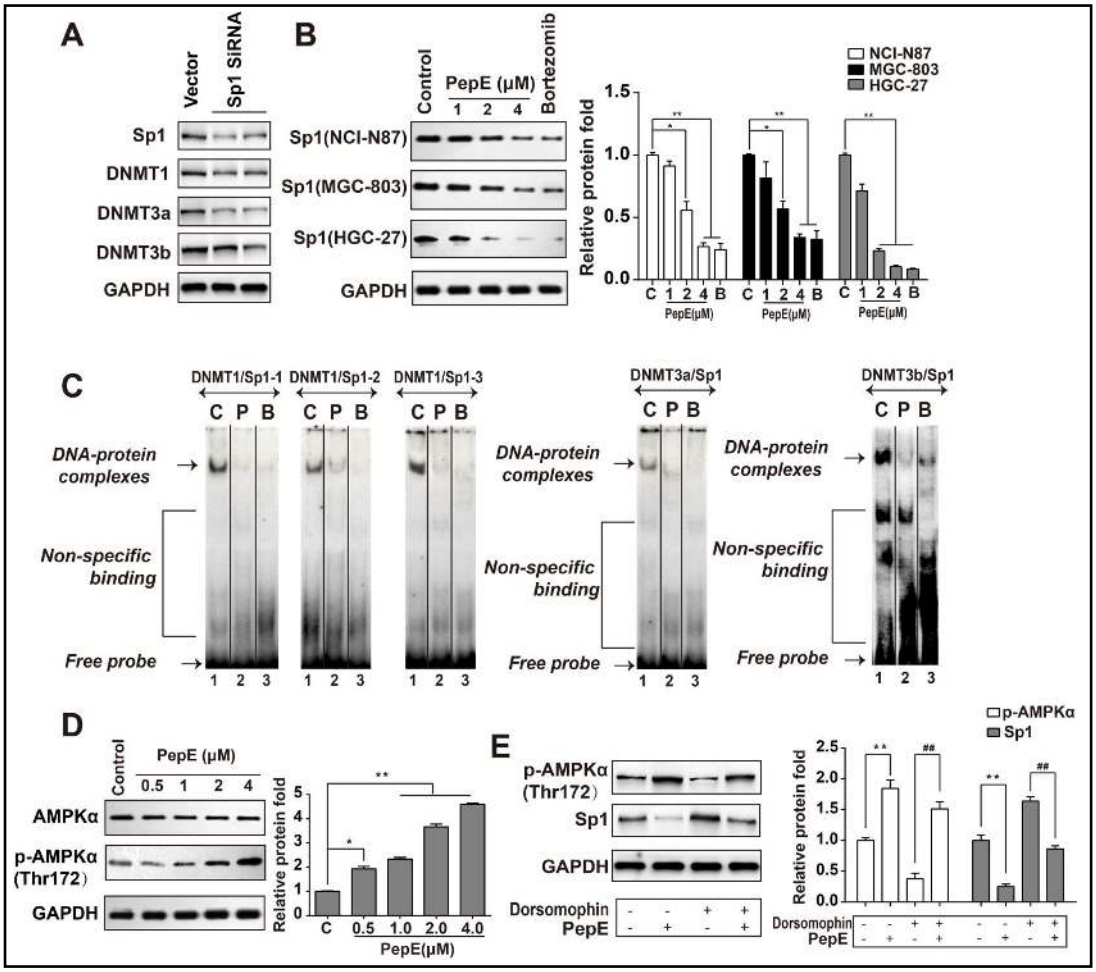

Fig. 8. PepE inhibits AMPKα-Sp1-DNMT signaling in GC cells. (A) Sp1 siRNA concurrently decreased Sp1 and DNMTs (including DNMT1, 3a and 3b) expression in NCI-N87 cells. NCI-N87 cells were transfected with negative control SiRNA (vector) or Sp1 siRNA (1 or 2) and cultured for 2 weeks. Total cell lysates were subjected to Western blot for Sp1, DNMT1, 3a and 3b. (B) PepE inhibits Sp1 protein expression in GC cells. Reduced Sp1 expression in NCI-N87, MGC-803 and HGC-27 cells treated with indicated dosage of PepE for 24 h. Bortezomib was used as positive control (C:control, B:Bortezomib, 100 nM). Data are presented as mean ± SD (n=3), *P<0.05; **P<0.01. (C) PepE abolished Sp1 binding to the DNMT1, 3a and 3b promoter. EMSA was performed with nuclear extracts prepared from NCI-N87 cells untreated or treated with PepE or bortezomib. The DNMT1/Sp1, DNMT3a/Sp1 and DNMT3b/Sp1 probes are shown on the top of each panel. C indicates control; P: PepE (2 μM), and B: bortezomib (100 nM). (D) PepE induced phosphorylation of AMPKα in NCI-N87 cells at indicated doses for 24 h. Data are presented as mean ± SD (n=3). *P<0.05; **P<0.01 when compared with control. (E) The inhibition ability of PepE against Sp1 expression was abrogated by dorsomophin (an AMPK inhibitor). NCI-N87 cells were treated with dorsomophin (10 μM) for 2 h before exposure of the cells to PepE (4 μM) for an additional up to 24 h. Afterward, the expression of p-AMPKα and Sp1 were detected by Western blot. Data are presented as mean ± SD (n=3). **P<0.01 when compared with control, ##P<0.01 when compared with NCI-N87 cells only treated with dorsomophin.

the involvement of AMPK signaling in the regulation of Sp1 in GC cells. As shown in Fig. 8E, AMPK inhibitor (dorsomophin) treatment significantly reduced the level of p-AMPKα, which was found to dramatically increase the Sp1 protein expression in NCI-N87 cells; this activity was significantly attenuated in PepE-treated cells. The above all results suggested that PepE treatment led to the activation of p-AMPK, which in turn resulted in the down-regulation of Sp1 protein level and subsequent suppression of DNMT1 expression.

Decreases in DNMT1 transcription correlate with a decrease in migration and invasion of GC cells

To further elucidate the role of DNMT1 as the mediating factor in GC metastasis, a knock-down of DNMT1 with siRNA was executed in NCI-N87 cells (Fig. 9A). As shown in Fig. 9B-C, DNMT1 knock-down significantly suppressed the cell migration and invasion in GC cells, which was similar to the effect of PepE. Moreover, our results demonstrated that 5-Aza-dC, a typical nucleotide DNMT1 inhibitor, also prevented the migration and invasion of NCI-N87 cells. Therefore, the above data suggested that the activity and expression of DNMT1 could directly regulate the metastasis of GC cells.

PepE treatment in GC cells reduces global DNA methylation in vitro and in vivo, thereby increasing expression of epigenetically silenced invasion-suppressor genes

Given the inhibitory effects of PepE on DNMT activity and transcription, we next investigated whether this compound also induced DNA hypomethylation. NCI-N87, MGC-803, and HGC-27 cells were treated with 0.5, 1.0, 2.0, or 4.0 μM of PepE or 1.0 μM of 5-Aza-dC for 24 h. Genomic DNA was isolated, hydrolyzed, and assessed for the levels of global DNA methylation by ultra-fast liquid chromatography-tandem mass spectrometry according to previous report [52]. Typical multiple monitoring ion chromatograms for dG and 5-mdC are shown in Fig. 10A. Calibration curves of 5-mdC and dG are shown in Fig. 10B (R^2 = 0.9993).

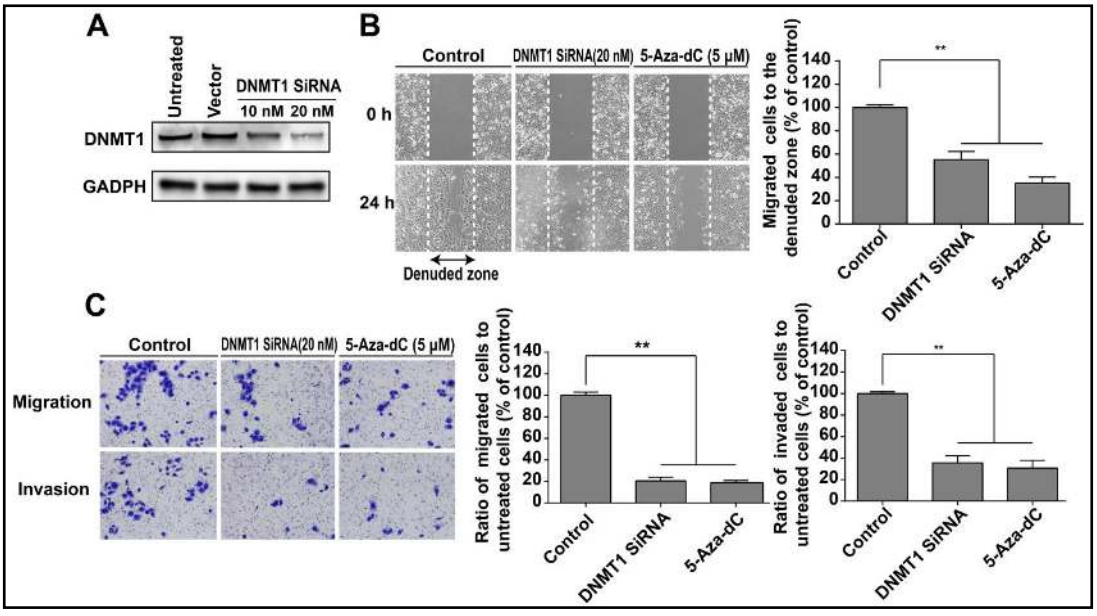

Fig. 9. Effects of DNMT1 inhibition on suppressing the metastasis of GC cells. (A) DNMT1 siRNA decreased DNMT1 expression in NCI-N87 cells dose dependently. (B) Wound healing assay of NCI-N87 before and after DNMT1 transcription decreased by SiRNA and inhibited by 5-Aza-dC. Histograms showed the ratio of migrated cells to the denuded zone of PepE treated cells when compared with control. (C) Migration and invasion assays of NCI-N87 before and after DNMT1 transcription decreased by SiRNA and inhibited by 5-Aza-dC. Histograms showed the ratio of migration cells and invasion cells of SiRNA and 5-Aza-dC group when compared with control. Cell numbers were counted in five randomly selected microscopic fields. All the above data is shown as mean ± SD of three independent experiments. *P<0.05; **P<0.01.

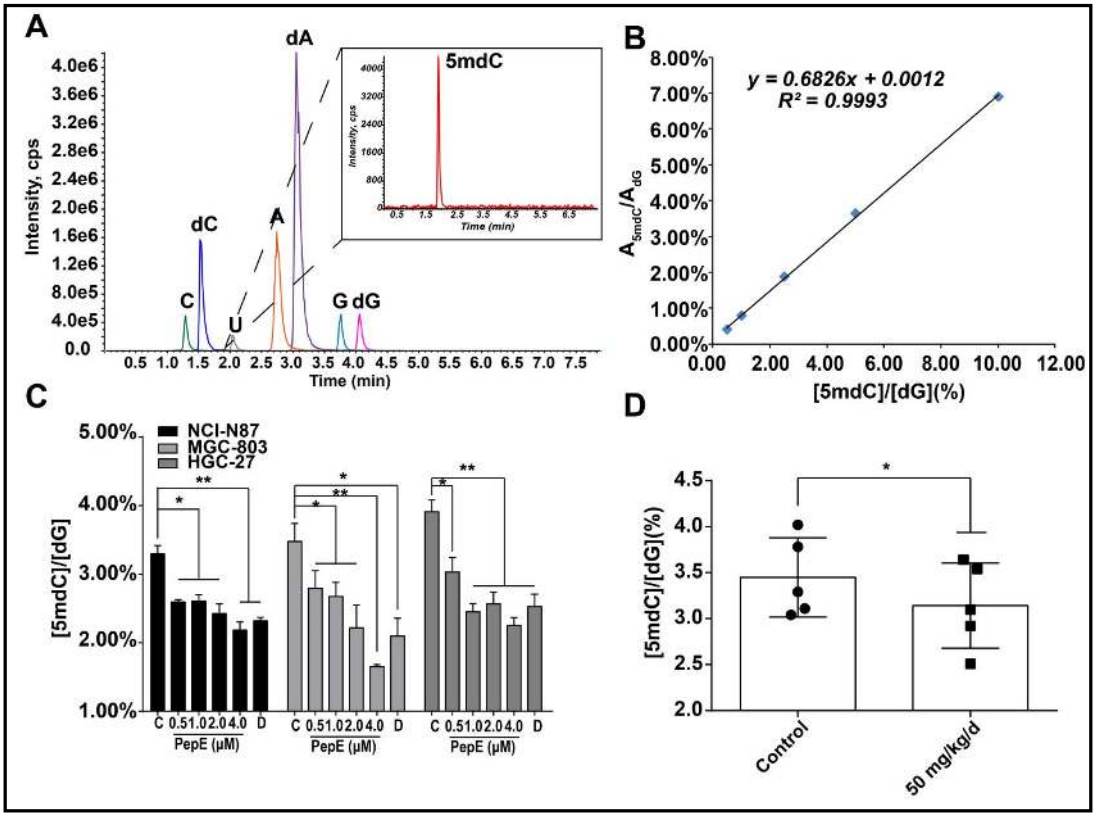

Fig. 10. Effect of PepE on global DNA methylation in GC cells in vitro and in vivo. (A) Represent chromatogram using ultra-fast liquid chromatography tandem mass spectrometry of 5-methyl-deoxycytidine (5mdC) and deoxyguanosine (dG) in DNA of hydrolyzed NCI-N87 cells. (B) Calibration curve between the peak area ration of 5mdC to dG (A_{5mdC}/A_{dG}) versus [5mdC]/[dG]%. (C) Effects of PepE and 5-Aza-dC on global DNA methylation levels in GC cells (C: control, D: 5-Aza-dC). (D) Effcts of PepE on the global DNA methylation levels in NCI-N87 tumor tissues extracted from NOD-SCID mice. Data are presented as mean ± SD (n=3 for C, n=5 for D), *P<0.05; **P<0.01.

As shown in Fig. 10C, DNA methylation levels in GC cells treated with PepE and 5-Aza-dC were significantly lower than those in the untreated controls. Especially in MGC-803 cells, approximately 50% reduction in global DNA methylation was observed in PepE-treated (4.0 μM) cells compared with the untreated control. To test whether this effect could be reduced *in vivo*, DNA samples from NCI-N87 tumor tissues extracted from the nude mice were also analyzed by this methodology. We observed significant DNA hypomethylation in the tumor tissues from PepE-treated group compared with negative controls (P<0.05). This effect correlated with the aforementioned changes in DNMT activity and protein levels, suggesting that PepE acted as a hypomethylator both *in vitro* and *in vivo* by down-regulating DNMTs.

The E-cadherin gene (also known as *CDH1*) is located on chromosome 16q22.1. E-cadherin constitutes an important invasion-suppressor gene that is frequently methylated and silenced in several cancers, especially in the poorly differentiated GC and diffuse histotype. Moreover, E-cadherin methylation is associated with poor prognosis of patients with GC, emphasizing its potential clinical significance [32-43]. The *TIMP3* gene is related to tumor development, in particular antagonizing the activity of metalloproteinases as well as inhibiting tumor growth, invasion, and metastasis. It has been reported that TIMP3 plays an invasion-suppressor function in GC. Moreover, *TIMP3* is highly frequently methylated in GC cell lines and primary tumors, which leads to gene silencing. Notably, restoring TIMP3 expression in GC cells decreases tumor cell migration, further demonstrating its invasion-suppressor role in GC [44-47].

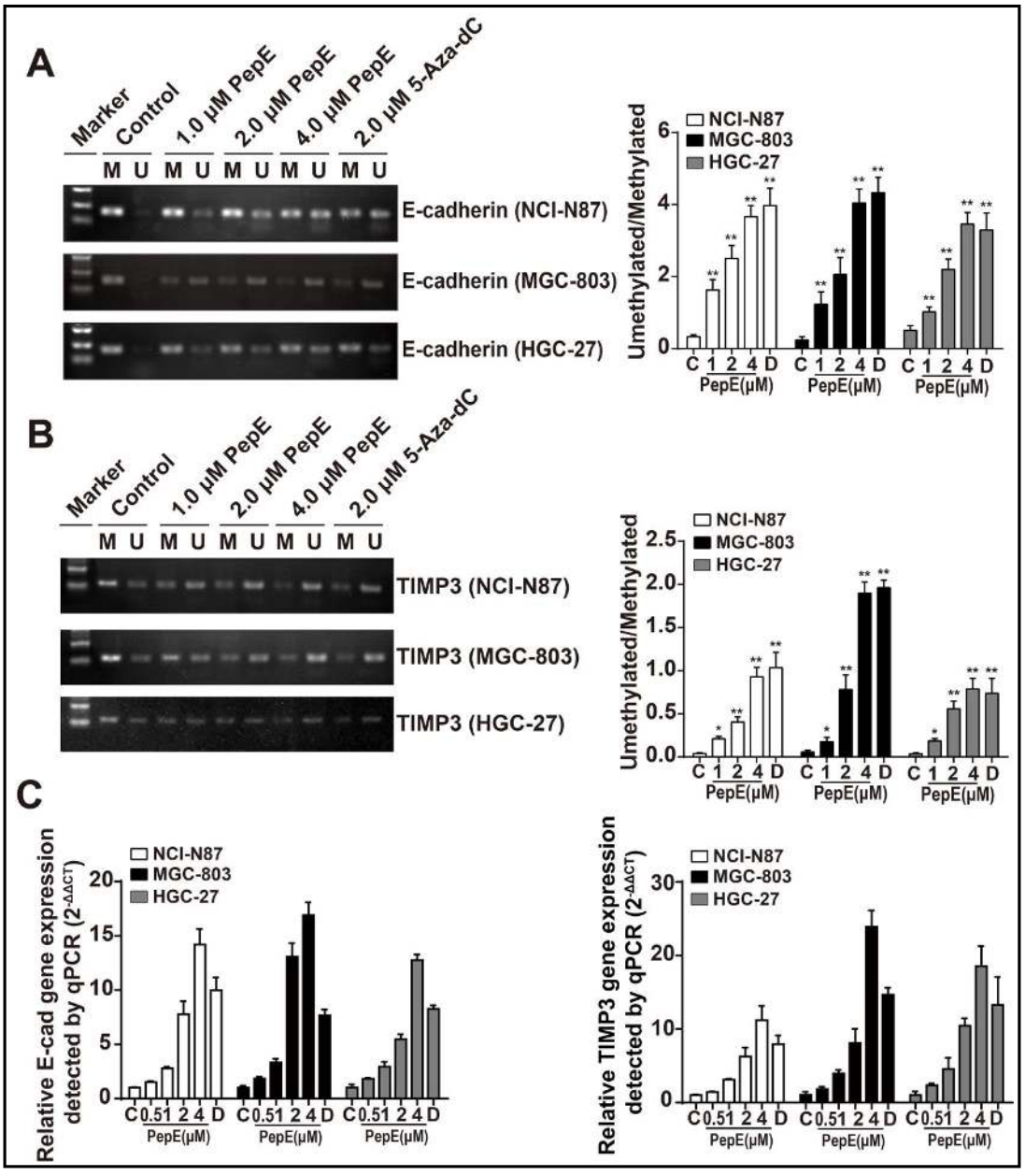

Fig. 11. Effects of PepE on the change of methylation status and gene expression of metastatic-suppressor genes (MSGs) in GC cells. (A) Methylation-specific PCR detected E-cadherin methylation status in NCI-N87, MGC-803 and HGC-27 cells before and after adding to different doses of PepE and 5-Aza-dC. (B) Methylation-specific PCR detected TIMP3 methylation status in NCI-N87, MGC-803 and HGC-27 cells before and after adding to different doses of PepE and 5-Aza-dC. (C) E-cadherin and TIMP3 genes' expression detected by RT-qPCR before and after PepE and 5-Aza-dC treatment. Data are presented as means ± SD (n=3), *P<0.05; **P<0.01. M: methylated; U: unmethylated; C: control; D: 5-Aza-dC.

As PepE inhibits DNMT activity and expression, we speculated that PepE might be involved in demethylation and reactivation of E-cadherin and *TIMP3* genes in GC cells. Therefore, we investigated the methylation status of E-cadherin and *TIMP3* genes in NCI-N87, MGC-803, and HGC-27 cells using methylation-specific PCR before and after PepE treatment. As expected, the E-cadherin gene was fully methylated in untreated NCI-N87, MGC-803, and HGC-27 cells, confirming its silenced state in these cell lines. Following 1 μM PepE treatment, noticeable increase in the levels of unmethylated E-cadherin level were observed, and after

2 or 4 μM treatment, this effect was even more significant ($P < 0.01$ when compared with untreated, Fig. 11A). Quantitative real-time PCR analysis revealed that PepE and 5-Aza-dC each reactivated silenced E-cadherin mRNA expression in a concentration dependent manner in NCI-N87, MGC-803, and HGC-79 cells, respectively (i.e., >14-fold for NCI-N87, >17-fold for MGC-803, and >13-fold for HGC-27 cells at 4 μM PepE, Fig. 11C by left). Similar findings were obtained for *TIMP3*. As shown in Fig. 11b, this gene was partially methylated in NCI-N87, MGC-803 and HGC-27 cells. After treatment of PepE, the level of unmethylated *TIMP3* was significantly increased in these cells ($P < 0.01$ when compared with untreated, Fig. 11B), The quantitative real-time PCR results demonstrated that the mRNA expression of *TIMP3* was significantly restored in a dose dependent manner following PepE treatment (i.e., >11-fold for NCI-N87, >23-fold for MGC-803, and >18-fold for HGC-27 cells at 4 μM PepE, Fig. 11C by right).

In vitro protein reactivation levels were determined using western blot analysis. As shown in Fig. 12A, PepE and 5-Aza-dC each significantly reactivated silenced E-cadherin in NCI-N87 cells in a concentration dependent manner. The protein levels of TIMP3 were also significantly restored in NCI-N87 cells in a dose dependent manner, followed by significant inhibition of a series of transduction signal proteins (MMP-2 and MMP-9) to elicit the anti-metastatic activity (Fig. 12A). Immunohistochemical analysis showed that there was a significant increase in E-cadherin and TIMP3-positive cells in the tumor tissues of PepE-treated mice when compared to the control group in NCI-N87 nude mice model ($P < 0.01$, Fig. 12B).

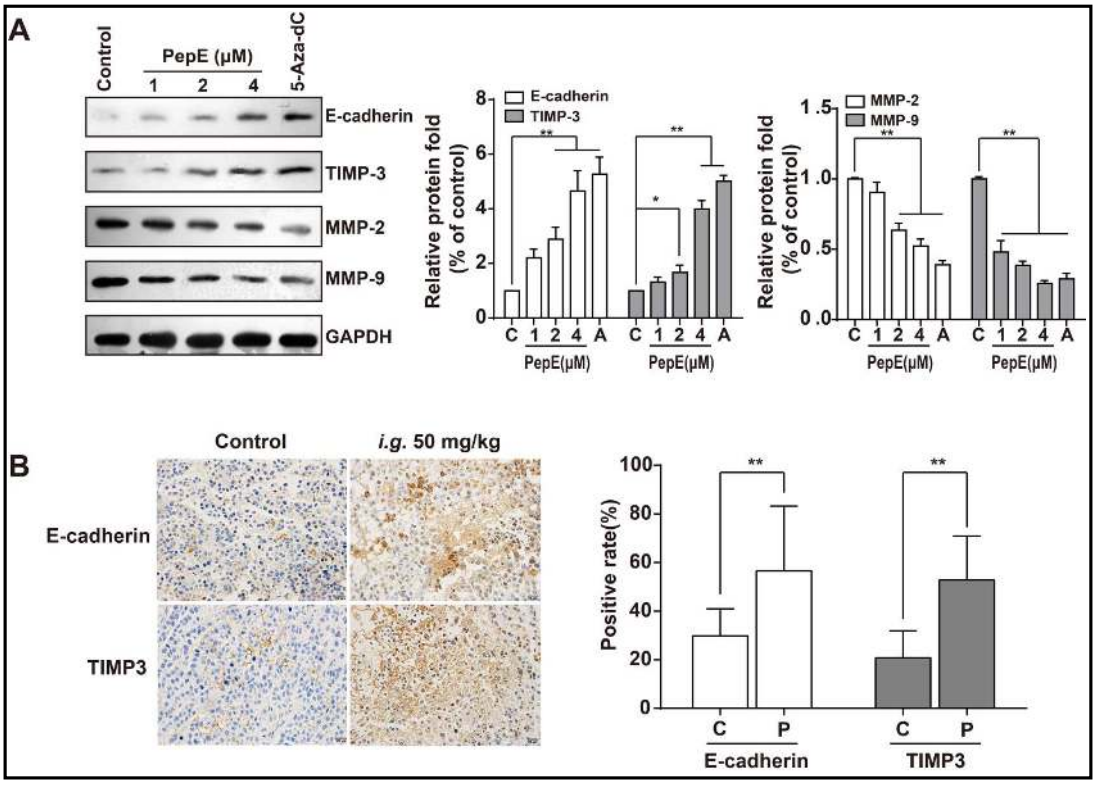

Fig. 12. Effects of PepE on the change of protein expression of epigenetically silenced MSGs in NCI-N87 cells in vitro and in vivo. (A) Western-blot bands for E-cadherin, TIMP3 and transduction signal proteins of TIMP3: MMP-2 and MMP-9 in NCI-N87 cells. The intensity of the bands was quantified by optical density (OD) and normalized to the OD of GAPDH. (B) Representative Immunostaining for E-cadherin and TIMP3 in the paraffin section (200 x) of tumors from in vivo anti-tumor experiment. 3 slides per mouse were reviewed. The positive rate was quantified by IOD values and normalized to the IOD values of control group. Data are presented as means ± SD (n=3 for A, n=5 for B), *P<0.05; **P<0.01.

Discussion

GC is characterized by rapid emergence of systemic metastases, resulting in poor prognosis owing to limited curative treatment options. As response rates to current cytotoxic agents (i.e., platinum and 5-fluorouracil) are rather low, the outlook for patients with metastatic GC is very poor, with median survival ranging from 4 to around 12 months [1, 3-5]. Therefore, finding a new therapy for metastatic GC from TCM may expand our understanding of this disease and allow the development of new therapeutic drugs. Notably, our results from this study provide strong evidence that PepE, a naturally derived secolignan from the Chinese anticancer folk medicine P. dindygulensis, can effectively suppress proliferation and invasion/migration of poorly-differentiated GC cells in vitro and in vivo with low toxicity against normal cells.

Inhibition of cell proliferation and induction of anti-metastatic activity are controlled by various genes (proteins) and signaling pathways. Among these, E-cadherin and TIMP3 have been frequently reported as the key metastasis suppressor genes in cancer cells, particularly in GC. Increasing evidence indicates that the gene promoters of E-cadherin and TIMP3 are frequently hypermethylated in poorly differentiated GC whereas DNMTs are over-expressed, which leads to reduced gene expression or even gene silencing [22-47]. Therefore, the inhibition of DNA methylation level is currently considered as a promising means of attenuating metastasis in human GC cells.

In the present study, we demonstrated that PepE is particularly effective in inhibiting DNMT1 activity (with IC_{50} at 3.61 μM, although it is not active against DNMT3a and 3b) through physically binding to the protein (with K_D value at 3.03 $x10^{-5}$ M). We then docked the compound to the catalytic pocket of DNMT1 and found that PepE could bind thereto, possibly in competition with cofactor SAH. Subsequently, the α-methylene-γ-lactone moiety of PepE may covalently bind with the thiol group of the Cys 1226 residue in the DNMT1 catalytic domain, thus inhibiting the enzyme activity. Furthermore, we also found in this study that PepE down-regulates the transcriptional level of DNMT1, 3a, and 3b, and inhibits their protein expression in a dose-dependent manner in tested GC cells. This occurs through disruption of the physical interaction of Sp1 with the DNMT1, 3a, and 3b promoter and through mediation of the AMPKα-Sp1 signaling pathway. Thus, the dual inhibitory activity of PepE; i.e., down-regulation of DNMT1, 3a, and 3b and covalent binding of the DNMT1 protein, underlies its comparable global DNA hypomethylation ability in the tested GC cell lines.

Notably, the global DNA methylation level of GC cells decreased significantly after exposure to PepE, with a similar in vivo hypomethylation activity in NCI-N87 orthotopic implantation NOD/SCID mice. Further examination of the reactivation of epigenetically reduced MSGs demonstrated that PepE also induces hypomethylation of the hypermethylated E-cadherin and TIMP3 gene promoters and enhances their expression in MGC-803, NCI-N87, and HGC-27 cells. Thus, it was clear that PepE blocks cell invasion and metastasis by epigenetic inhibition of DNMT function and reactivation of the hypermethylated MSGs in GC cells.

Over the past decades, two types of DNMT inhibitors have been discovered: nucleoside analogs and non-nucleoside compounds [59]. The former have been approved by the US Food and Drug Administration for the treatment of myelodysplastic syndrome and leukemia (i.e., 5-Aza-dC). However, such analogs need to be incorporated into DNA and serve as covalent inhibitors, with poor chemical stability, low specificity, and significant toxic side effects. In contrast, the non-nucleoside compounds with various chemical scaffolds have recently attracted much attention. Several natural products, such as genistein, laccaic acid A, and (-)-epigallocatechin-3-O-gallate (EGCG), were reported to inhibits DNMT activity. Unfortunately, the potency of these compounds is lower than that of the nucleoside analogs and their in vivo inhibitory activity against solid tumors is rarely reported [60-61]. This situation prompts an urgent need to discover new-generation DNMT inhibitors with high in vitro and in vivo potency against tumors.

Conclusion

Together, the findings of this study highlight PepE as an effective DNA methylation inhibitor via its dual functions of potentially binding to the catalytic site of DNMT1 and down-regulating the expression levels of DNMT1, 3a, and 3b through AMPKα-Sp1-DNMTs signaling (Fig. 13). Thus, PepE appears to constitute a putative new-generation DNMT inhibitor as well as being a promising lead compound for the intervention of GC invasion/migration. Moreover, the findings are of importance for understanding the mechanisms of PepE anti-metastatic activity against GC cells. Further studies regarding the detailed mechanism of anticancer activity and structural modification analyses to increase the efficacy of this agent are ongoing.

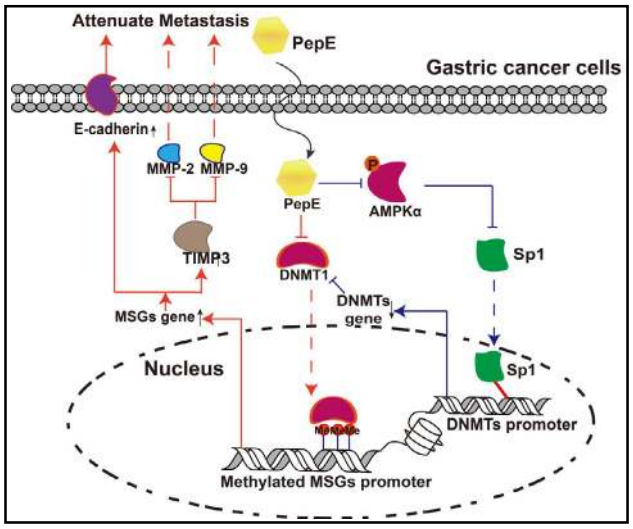

Fig. 13. The proposed signaling pathways for PepE-inhibited migration and invasion of poorly differentiated GC cells.

Abbreviations

3D (three-dimensional); BLI (bio-layer Interferometry); DMSO (dimethylsulfoxide); DNMT (DNA methyltransferase); EMSA (electrophoretic mobility-shift assay); FBS (fetal bovine serum); GC (gastric cancer); MMP (metalloproteinase); PBS (phosphate buffered saline); PepA (Peperomin A); PepE (Peperomin E); 5-Aza-dC (Decitabine); SA (streptavidin); SAH (S-adenosyl-L-homocysteine); siRNA (small interfering RNA); TCM (traditional Chinese medicine); TIMP (tissue inhibitor of metalloproteinases).

Acknowledgements

This work was funded by Grants from the Natural Science Foundation of China (No. 81402812), the Natural Science Foundation of Jiangsu Province (No. BK20130954) and the Priority Academic Program Development of Jiangsu Higher Education Institutions.

Disclosure Statement

The authors declare that there is no duality of interest associated with this manuscript.

References

1 Cutsem EV, Sagaert X, Topal B, Haustermans K, Prenen H: Gastric cancer. Lancet 2016;388:2654-2664.
2 Shen L, Shan YS, Hu HM, Price TJ, Sirohi B, Yeh KH, Yang YH, Sano T, Yang HK, Zhang XT: Management of gastric cancer in Asia: resource-stratified guideline. Lancet Oncol 2014;14:535-547.
3 Ushijima T, Sasako M: Focus on gastric cancer. Cancer Cell 2004;5:121-125.
4 Duraes C, Almeida GM, Seruca R, Oliveira C, Carneiro F: Biomarkers for gastric cancer: prognostic, predictive or targets of therapy? Virchows Arch 2014;464:367-378.

5 Karimi P, Islami F, Anandasabapathy S, Freedman ND, Karmangar F: Gastric cancer: descriptive epidemiology, risk factors, screening and prevention. Cancer Epidem Biomar Prev 2014;23:700-713.
6 Li X, Yang GY, Li XX, Zhang Y, Yang JL, Chang J, Sun XX, Zhou XY, Guo Y, Xu Y: Traditional Chinese Medicine in cancer care: a review of controlled clinical studies published in Chinese. Plos One 2013;8:60338-60340.
7 Efferth T, Li PCH, Konkimalla VSB, Kaina B: From Traditional Chinese medicine to rational cancer therapy. Trends Mol Med 2007;13:353-360.
8 Xu Y, Zhao GA, Li ZY, Zhao G, Cai Y, Zhu XH, Cao ND, Yang JK, Zhang J, Gu Y: Survival benefit of traditional Chinese herbal medicine for patients with advance gastric cancer. Integr Cancer Ther 2012;12:414-422.
9 Lin CQ, Yue XQ, Ling C: Three advantages of using traditional Chinese medicine to prevent and treat tumor. J Integr Med 2014;12:331-335.
10 Liu X, Xiu LJ, Jiao JP, Zhao J, Zhao Y, Lu Y, Shi J, Li YJ, Ye M, Gu YF: Traditional Chinese medicine integrated with chemotherapy for stage IV non-surgical gastric cancer: a retrospective clinical analysis. J Integr Med 2017;15:469-475.
11 Tan W, Lu JJ, Huang MQ, Li YB, Chen MW, Wu GS, Gong J, Zhong ZF, Xu ZT, Dang YY: Anti-cancer natural products isolated from Chinese medicinal herbs. Chin Med 2011;6:27.
12 Ministry of Health of Kunming Military Region Logistics Department: Selection of Chinese herbal medicine in Yunnan; ed 1, Tianjin People's Printing Press, Tianjing, 1970.
13 Govindachari TR, Krishna Kumari GN, Partho PD: Two secolignans from *Peperomia dindygulensis*. Phytochem 1998;49:2129-2131.
14 Wu JL, Li N, Hasegawa T, Sakai J, Mitsui T, Ogura H, Kataoka T, Oka S, Kiuchi M, Tomida A: Bioactive secolignans from *Peperomia dindygulensis*. J Nat Prod 2006;69:790-794.
15 Wu JL, Li N, Hasegawa T, Saikai J, Kakuta S, Tang WX, Oka S, Kiuchi M, Ogura H, Kataoka T: Bioactive tetrahydrofuran lignans from *Peperomia dindygulensis*. J Nat Prod 2005;68:1656-1660.
16 Chen L, Zhou Y, Dong JX: Three new flavonoid glycosides from *Peperomia dindygulensis*. Acta Pharm Sin 2007;42:183-186.
17 Wang QW, Yu DH, Lin MG, Zhao M, Zhu WJ, Lu Qin, Li GX, Wang C, Yang YF, Qin XM, Fang C, Chen HZ, Yang GH. Antiangiogenic polyketides from *Peperomia dindygulensis* Miq. Molecules 2012;17:4474–4483.
18 Wang XZ, Qu W, Liang JY. New long-chain aliphatic compounds from *Peperomia dindygulensis*. Nat Prod Res 2013;27:796–803.
19 Xu S, Li N, Ning MM, Zhou CH, Yang QR, Wang MW. Bioactive compounds from *Peperomia pellucida*. J Nat Prod 2006;69:247-250.
20 Tsutsui C, Yamada Y, Ando M, Toyama D, Wu JL, Wang LY, Taketani S, Kataoka T: Peperomins as anti-inflammatory agents that inhibit the NF-kappa B signaling pathway. Bioorg Med Chem Lett 2009;19:4084-4087.
21 Wang XZ, Cheng Y, Wu H, Li N, Liu R, Yang XL, Qiu YY, Wen HM, Liang JY: The natural secolignan peperomin E induces apoptosis of human gastric carcinoma cells via the mitochondrial and PI3K/Akt signaling pathways *in vitro* and *in vivo*. Phytomed 2016;23:818-827.
22 Mclean MH, El-Omar EM: Genetics of gastric cancer. Nature Rev Gastr Hepat 2014;11:664-674.
23 Li Y, Liang J, Hou P: Hypermethylation in gastric cancer. Clin Chim Acta 2015;448:124-132.
24 Ding WJ, Fang JY, Chen XY, Peng YS: The expression and clinical significance of DNA methyltransferase proteins in human gastric cancer. Dig Dis Sci 2008;53:2083-2089.
25 Mutze K, Langer R, Schumacher F, Becker K, Ott K, Novotny A, Hapfelmeier A, Hofler H, Keller G: DNA methyltransferase 1 as a predictive biomarker and potential therapeutic target for chemotherapy in gastric cancer. Eur J Cancer 2011;47:1817-1825.
26 Choi SJ, Shin YS, Kang BW, Kim JG, Won KJ, Lieberman PM, Cho H, Kang H: DNA hypermethylation induced by Epstein-Barr virus in the development of Epstein-Barr virus-associated gastric carcinoma. Arch Pharm Res 2017;40:894-905.
27 Robert MF, Morin S, Beaulieu N, Gauthier F, Chute IC, Barsalou A, MacLeod AR: DNMT1 is required to maintain CpG methylation and aberrant gene silencing in human cancer cells. Nat Genet 2003;33:61-65.
28 Yamashita S, Tsujino Y, Moriguchi K, Tatematsu M, Ushijima T: Chemical genomic screening for methylation-silenced genes in gastric cancer cell lines using 5-aza-2'-deoxycytidine treatment and oligonucleotide microarray. Cancer Sci 2006;97:64-71.

29 Chang MS, Uozaki H, Chong JM, Ushiku T, Sakuma K, Ishikawa S, Hino R, Barua RR, Iwasaki Y, Arai K: CpG island methylation status in gastric carcinoma with and without infection of Epstein-Barr virus. Clin Cancer Res 2006;12:2995-3002.
30 House M. Tumor suppressor gene hypermethylation as a predictor of gastric stromal tumor behavior. J Gastroint Surg 2003;7:1004-1014.
31 Zhao C, Bu X: Promoter methylation of tumor-related genes in gastric carcinogenesis. Histol Histopathol 2012;27:1271-1282.
32 Hirohashi S: Inactivation of the E-Cadherin-Mediated cell adhesion system in human cancers. American J Pathol 1998;153:333-339.
33 Tanaka M, Kitajima Y. Edakuni G, Sato S, Miyazaki K: Abnormal expression of E-cadherin and β-catenin may be a molecular marker of submucosal invasion and lymph node metastasis in early gastric cancer. Brit J Surg 2002;89:236-244.
34 Onder TT, Gupta PB, Mani SA, Yang J, Lander ES, Weinberg RA: Loss of E-cadherin promotes metastasis via multiple downstream transcriptional pathways. Cancer Res 2008;68:3645-3654.
35 Li XW, Shi BY, Yang QL, Wu J, Wu HM, Wang YF, Wu ZJ, Fan YM, Wang YP: Epigenetic regulation of CDH1 exon 8 alternative splicing in gastric cancer. BMC Cancer 2015;15:954.
36 Huang FY, Chan AO, Rashid A, Wong DK, Cho CH, Yuen MF: Helicobacter pylori induces promoter methylation of E-cadherin via interleukin-1beta activation of nitric oxide production in gastric cancer cells. Cancer 2012;118:4969-4980.
37 Chan OOA, Lam SK, Wang BCY, Wong WM, Yuen MF, Yeung YH, WM Hui, Rashid A, Kwong YL: Promoter methylation of E-cadherin gene in gastric mucosa associated with Helicobacter pylori infection and in gastric cancer. Gut 2003;52:502-506.
38 Graziano F. Combined analysis of E-cadherin gene (CDH1) promoter hypermethylation and E-cadherin protein expression in patients with gastric cancer: implications for treatment with demethylating drugs. Annal Oncol 2004;15:489-492.
39 Huang FY, Chan AO, Rashid A, Wong DK, Cho CH, Yuen MF: Helicobacter pylori induces promoter methylation of E-cadherin via interleukin-1beta activation of nitric oxide production in gastric cancer cells. Cancer 2012;118:4969-4980.
40 Pharoah PDP, Guilford P, Caldas C: Incidence of gastric cancer and breast cancer in CDH1 (E-cadherin) mutation carriers from hereditary diffuse gastric cancer families. Gastroenter 2001;121:1348-1353.
41 Grady WM, Willis J, Guilford PJ, Dunbier AK, Toro TT, Lynch H, Wiesner G, Fergusen K, Eng C, Park JG, SJ Kim, Markowitz S: Methylation of the CDH1 promoter as the second genetic hit in hereditary diffuse gastric cancer. Nature Genet 2000;26:16-17.
42 Yoshiura K, Kanai Y, Ochiai A, Shimoyama Y, Sugimura T, Hirohashi S: Silencing of the E-cadherin invasion-suppressor gene by CpG methylation in human carcinomas. Proc Natl Acd Sci USA 1995;92:7416-7419.
43 Moghbeli M, Moaven O, Memar B, Raziei HR, Aarabi A, Dadkhah E, Forghanifard MM, Manzari F, Abbaszadegan MR. Role of hMLH1 and E-cadherin promoter methylation in gastric cancer progression. J Gastrointest Cancer 2014;45:40-47.
44 Guan ZY, Zhang J, Song SH, Dai DQ: Promoter methylation and expression of TIMP3 gene in gastric cancer. Diagn Pathol 2013;8:110-116.
45 Guo MZ, Yan WJ: Epigenetics of Gastric Cancer; in (Verma M, ed) eds, Cancer Epigenetics, Berlin, Springer, 2014, vol.5, pp. 783-799.
46 Kubben FJGM, Sier CFM, Meijer MJW, Berg MVD, Reijden JJVD. Griffioen G, Velde JHVD, Lamers CBHW, Verspaget HW: Clinical impact of MMP and TIMP gene polymorphisms in gastric cancer. Brit J Cancer 2006;95:744-751.
47 Joo YE, Seo KS, Kim HS, Rew JS, Park CS, Kim SJ: Expression of tissue inhibitors of metalloproteinases in gastric cancer. Dig Dis Sci 2000;45:114-121.
48 Liu KC, Huang AC, Wu PP, Lin HY, Chueh FS, Yang JS, Liu CC, Chiang JH, Meng MS, Chung JG: Gallic acid suppress the migration and invasion of PC-3 human prostate cancer cells via inhibition of matrix metalloproteinase-2 and -9 signaling pathways. Oncol Rep 2011;26:177-184.
49 Liu SJ, Liu ZF, Xie ZL, Pang JX, Yu JH, Lehmann E, Huynh L, Vukosavijevic T, Takeki M, Kilsovic RB: Bortezomib induces DNA hypomethylation and silenced gene transcription by interfering with Sp1/NF-κB-dependent DNA methyltransferase activity in acute myeloid leukemia. Blood 2008;111:2364-2673.

50 Kishikawa S, Murata T, Kimura H, Shiota K, Yokoyama KK: Regulation of transcription of the DNMT1 gene by Sp1 and Sp3 zinc finger proteins. FEBS J 2002;269:2961-2970.
51 Jinawath A, Miyake S, Yanagisawa Y, Akiyama Y, Yuasa Y: Transcriptional regulation of the human DNA transferase 3A and 3B genes by Sp3 and Sp1 zinc finger proteins. Biochem J 2005;385:557-564.
52 Song LG, James SR, Kazim L: Specific method for the determination of genomic DNA methylation by liquid chromatography-electrospray ionization tandem mass spectrometry. Anal Chem 2005;77:504-510.
53 Yuan YT: Establishment of animal model of gastric carcinoma in situ with lymph node metastasis. Master dissertation of Nanjing University 2016;1:12-14.
54 Zhang S: Effect of Xiaotan Sanjie Recipe on the Metastasis of Human gastric carcinoma and related adhesion molecule in orthotopic implantation nude mice mode. Doctoral dissertation of Secondary Military Hospital 2005;1:16-19.
55 Wang XZ, Cheng Y, Wang KL, Liu R, Yang XL, Wen HM, Chai C, Liang JY, Wu H: Peperomin E reactivates silenced tumor suppressor genes in lung cancer cells by inhibition of DNA methyltransferase. Cancer Sci 2016;107:1506-1519.
56 Liu ZF, Liu SJ, Xie ZL, Pavlovicz RE, Wu JJ, Chen P, Aimiuwu J, Pang JX, Bhasin D, Neviani P: Modulation of DNA methylation by a sesquiterpene lactone parthenolide. J Pharmacol Exper Ther 2009;329:505-514.
57 Zhao S, Wu J, Tang Q, Zheng F, Yang L, Chen Y, Li L, Hann SS: Chinese herbal medicine Xiaoji decoction inhibited growth of lung cancer cells through AMPKalpha-mediated inhibition of Sp1 and DNA methyltransferase 1. J Ethnopharmacol 2016;181:172-181.
58 Yie Y, Zhao S, Tang Q, Zheng F, Wu J, Yang L, Deng S, Hann SS: Ursolic acid inhibited growth of hepatocellular carcinoma HepG2 cells through AMPKalpha-mediated reduction of DNA methyltransferase 1. Mol Cell Biochem 2015;402:63-74.
59 Brueckner B, Lyko F: DNA methyltransferase inhibitors: old and new drugs for an epigenetic cancer therapy. TRENDS Phamacol Sci 2004;25:551-554.
60 Gnyszka A, Jastrzebski Z, Flis S: Role in epigenetic therapy of cancer. Anticancer Res 2013;33:2989-2996.
61 Xu P, Hu G, Luo C, Liang ZJ: DNA methyltransferase inhibitors: an updates patent review (2012-2015). Exp Opin Ther Pat 2016;26:1017-1030.